fire

MDPI

Article

A New Perspective on Hydrogen Chloride Scavenging at High Temperatures for Reducing the Smoke Acidity of PVC Cables in Fires, IV: The Impact of Acid Scavengers at High Temperatures on Flame Retardance and Smoke Emission

Iacopo Bassi [1], Francesca Delchiaro [1], Claudia Bandinelli [1], Laura Mazzocchetti [2], Elisabetta Salatelli [2] and Gianluca Sarti [1,*]

[1] Reagens S.p.A., Via Codronchi, 4, 40016 San Giorgio di Piano, Italy; iacopo.bassi@reagens-group.com (I.B.); francesca.delchiaro@reagens-group.com (F.D.); claudia.bandinelli@reagens-group.com (C.B.)
[2] Department of Industrial Chemistry "Toso Montanari", University of Bologna, Viale Risorgimento 4, 40136 Bologna, Italy; laura.mazzocchetti@unibo.it (L.M.); elisabetta.salatelli@unibo.it (E.S.)
* Correspondence: gianluca.sarti@fastwebnet.it

Abstract: In PVC compounds, hydrogen chloride plays a fundamental role in ·H and ·OH radical trapping, lowering the flame energy during combustion. Furthermore, it yields actual Lewis acids promoting the cross-linking of the polyene sequences from PVC degradation and bringing a char layer, protecting PVC items from flames. Therefore, PVC is inherently flame-retarded. However, plasticized PVC requires flame retardants and smoke suppressants to enhance fire performance. Low-smoke acidity PVC compounds have been developed to reduce the HCl emission during combustion and, therefore, the acidity of the smoke. They contain potent acid scavengers capable of acting at high temperatures. They react with hydrogen chloride in the condensed phase, making it unavailable in the gas and even in the condensed phase, compromising the reaction to fire and enhancing the smoke produced during the combustion. The effect of the sequestration of hydrogen chloride in PVC compounds for cables by potent acid scavengers is studied in this paper through measurements of oxygen index, heat release, and smoke production. It is noteworthy that the potent acid scavengers strongly affect parameters such as the oxygen index, the fire growth rate in cone calorimetry, the specific (total) heat capacity, and the specific heat of combustion of fuel gases in micro combustion calorimetry. In some formulations, acid scavengers reduce the oxygen index below the values of the formulations without flame retardants and double their fire growth rate. In fact, they neutralize the action of antimony trioxide and Lewis acid precursors commonly used as flame retardants and smoke suppressants in PVC items, making them prone to ignite, release smoke, and spread flame. A new generation of flame retardants and smoke suppressants is needed to keep together the low-smoke acidity and the fire performance in PVC items.

Keywords: acid scavengers; PVC; cables; smoke acidity

Citation: Bassi, I.; Delchiaro, F.; Bandinelli, C.; Mazzocchetti, L.; Salatelli, E.; Sarti, G. A New Perspective on Hydrogen Chloride Scavenging at High Temperatures for Reducing the Smoke Acidity of PVC Cables in Fires, IV: The Impact of Acid Scavengers at High Temperatures on Flame Retardance and Smoke Emission. *Fire* **2023**, *6*, 259. https://doi.org/10.3390/fire6070259

Academic Editors: Ying Zhang, Xiaoyu Ju, Xianjia Huang and Fuchao Tian

Received: 6 June 2023
Revised: 24 June 2023
Accepted: 27 June 2023
Published: 30 June 2023

1. Introduction

1.1. Thermal Degradation, Thermal Decomposition, Pyrolysis, and Combustion: The Basic Concepts

The thermal degradation of unstabilized PVC starts at 100 °C [1] through zip elimination bringing polyene sequences and emitting hydrogen chloride (HCl). Most scientists consider the mechanism of PVC degradation ionic, and the resin defects and radicals play a fundamental role in lowering its thermal stability [2–6]. PVC cannot be processed in articles without additives preventing its thermal degradation. Moreover, additives must also give the final items the characteristics they need for the specific application, such as, among others, good weathering performances, aging resistance, and flame retardance.

Additive-containing PVC formulations are called PVC compounds. Due to PVC's low thermal stability, the main additives are thermal stabilizers. They delay the degradation processes induced by temperature and shear and shift them to higher temperatures, allowing the processing of PVC compounds at 150–220 °C. Primary stabilizers substitute the weakest moiety of the chain, the allylic chloride, forming a stronger bond with carbon than chlorine itself. They also contain co-stabilizers, helping the primary stabilizers in the chlorine displacement, blocking the action of byproducts or radicals speeding the zip elimination, and/or shortening the polyene sequences from the zip elimination of HCl. Co-stabilizers can have a preventive action, inhibiting the behavior of those substances, which increases the speed of the HCl elimination or curative activity when a repairing action of polyene sequences is involved.

Fires and their consequences differ depending on their heat flow, temperatures reached, ventilation, and mass of burning materials. After the ignition, i.e., the initial stage where temperatures are around 300–400 °C, if not inhibited, fire enters a stage where temperatures easily reach 600 °C and further its fully developed stage, easily overcoming 600 °C [7].

The heat released in fires brings physical and chemical changes to PVC items, causing thermal decomposition and combustion. PVC, stabilizers, co-stabilizers, plasticizers, lubricants, impact modifiers, processing aids, pigments, fillers, flame retardant fillers, flame retardants, and light stabilizers start all to decompose in the condensed phase or evaporate, releasing gaseous byproducts directly in the gas phase, where combustible fuels burn. Without the protection of stabilizers, PVC resin rapidly changes its chemical nature, forming polyene sequences, developing smoke, creating a char from cross-linked polyene sequences, and releasing massive amounts of HCl. Thermal decomposition and the involved species play a fundamental role in the combustion of PVC items, and knowing the underlying chemistry of such processes is crucial to address the reduction of heat, smoke, and gases such as HCl.

Several authors carried out different techniques to study PVC decomposition. Flash pyrolysis coupled with gas chromatography (GC), direct pyrolysis in the mass spectrometer (MS), and thermal gravimetric analysis (TGA) in different atmospheres and with different detection methods of the gases brought different interpretations of the reactions involved in the thermal decomposition of PVC [8–12]. TGA measures the weight loss, and if coupled with Fourier transform infrared (FTIR), MS, or GC-MS, the gases released during the decomposition can even be identified and quantified. Most scientists agree that PVC has two main stages during its decomposition. The first one refers to the zip elimination of HCl, the formation of the polyene sequences, their cross-linking, and the competitive reaction yielding benzene. The second relates to the decomposition of the cross-linked matrix to char residue and combustible fuels. Several additives commonly used in PVC compounds for processing or conferring specific properties further complicate the decomposition pattern and the involved reactions.

1.2. The First Stage of the Thermal Decomposition/Combustion

Performing a TGA of PVC in N_2, depending on heating regimes, highlights that the decomposition's first stage occurs between 220 °C and 350 °C. Here, HCl is released from the polymer's backbone, and polyene sequences are formed. Intramolecular reactions can bring the benzene formation [8,9,13], while intermolecular reactions lead to the cross-linking of the matrix [9,10,12,14]. At the end of the first stage, between 330 °C and 350 °C, when HCl is almost totally released, only the condensation products of the polyene sequences remain, and a plateau between 350 °C and 450 °C follows, with no volatile release.

However, PVC compounds contain additives such as stabilizers, plasticizers, flame retardants, and flame retardant fillers, and the types and their quantity can affect TGA shapes.

TGA and TGA-GC-MS or TGA-FTIR can highlight much about the decomposition of PVC compounds. Nevertheless, temperatures and physical and chemical properties are not the only parameters influencing fire behavior. Combustion is a complex phenomenon influenced by item shape and surrounding conditions such as oxygen concentration and

kind of ignition [15]. In any case, the combustion process implies two distinct categories of chemical reactions. The first happens in the condensed phase, where the oxygen concentration is low, and the thermal decomposition passes through a pyrolysis process, releasing volatile fuels. The second is the oxidation of the volatiles in the gas phase, producing the energy supporting the pyrolysis process.

In the first stage of thermal decomposition, PVC and the organic and inorganic additives in PVC items decompose thermally in a pyrolysis process where oxygen is starving. Depending on the ingredients in PVC compounds, different gases can be released at different rates. Some gases reaching the air burn, releasing energy and smoke. Others do not burn and dilute the fuels or cool the flame down. Organic substances and their byproducts can evaporate and burn in the flame: plasticizers [16], primary stabilizers and organic co-stabilizers, lubricants, processing aids, and many others can increase the heat release rate and the smoke production. Others, such as the water vapor from the thermal decomposition of flame retardant fillers such as magnesium dihydroxide (MDH) or aluminum trihydroxide (ATH), lower the flame's energy by acting as a heat sink diluting the fuels. Even side reactions between HCl and fillers such as calcium and magnesium carbonate can produce gases such as CO_2, weakening the flame. However, the main gas in the flame in this stage is HCl, released by the thermal decomposition of PVC. Here, the common acid scavengers used in the stabilizer one pack can no longer compete with the fast evolution of HCl in the gas phase.

HCl is not an inert gas such as water vapor or CO_2. Within the flame, it initiates a series of catalytic reactions capable of scavenging the radicals ·H and ·OH, lowering the flame's energy [17,18]. This phenomenon is called "the poisoning of the flame" and is the reason why all halogenated polymers are inherently flame-retardant. If Sb_2O_3 (ATO) is used, HCl also plays a central role in yielding $SbCl_3$. When it evaporates in the flame, it scavenges the hot radicals feeding the flame more efficiently than HCl alone, reducing its energy further [17,18].

The combustion in the flame can be seen as a competition between two reactions: the first brings the complete oxidation of the fuel when oxygen is rich and the flame is high in energy. The second happens when the flame's energy is low and oxygen starves. It causes a dehydrogenation of the organic substances in the fuel, releasing airborne water and carbon agglomerates we perceive as smoke. This last condition is reached when ATO is used, and items release massive smoke.

In the condensed phase, the polyene sequences formed during the zip elimination process can react intramolecularly (cis-olefinic structures), generating benzene, soot, and smoke, or intermolecularly (trans-olefinic structures) yielding cross-linked structures [9,10,12,13,18]. This last condition prevents smoke production. HCl is also crucial in the condensed phase, reacting with incipient Lewis acids commonly present in PVC smoke suppressants and forming actual Lewis acid, catalyzing the formation of trans-olefinic structures and promoting the intermolecular reaction yielding a cross-linked matrix and char. Therefore, HCl scavengers interfere with the smoke suppressant mechanism inhibiting smoke production.

1.3. The Second Stage of the Thermal Decomposition/Combustion

Performing a TGA of PVC in N_2, the second stage of the decomposition is over 450 °C. Here, the cross-linked matrix starts releasing volatiles (aliphatic hydrocarbons and alkylated aromatic) [12], leaving at the end carbonaceous char.

In a real fire scenario, the condensation products formed over 450 °C in PVC items release volatile fuels in the gas phase, and a carbonaceous char is formed in the condensed phase. The fuels burn, increasing the flame energy, and on the contrary, the formed carbonaceous char hampers the spread of the flame, creating a protective and insulating barrier. The char can be formed if oxygen is low in concentration in the gas phase, when temperatures are not so high as to bring it to complete combustion, or its thickness is so high that it hinders oxygen from permeating it entirely. However, the fuels released in this stage are mainly aliphatic moieties. They burn, releasing less smoke but more energy in the flame

than the aromatics in stage 1. The presence of Lewis acids coming from the typical smoke suppressants used in PVC items can even increase the quantity of those fuels in the gas phase because they promote the cationic crack of the char, and other strategies for avoiding this problem can be used [18–21]. When temperature increases over 600 °C and if oxygen is enough in the gas phase, the final step of the decomposition/combustion stage leads to the post-pyrolysis/combustion stage, where only ashes of oxides and chlorides remain.

Therefore, the thermal decomposition, released gases, and the gas- and condensed-phase reactions differ depending on the temperature, oxygen concentration, and the PVC compound's ingredients. Knowing the type of reactions in the flame and in the condensed phase is crucial to actively act to reduce the flame's energy, directly or indirectly, or to suppress smoke: that will have consequences on the fire performances of PVC items in terms of ignitability, flammability, flame spread, heat release, and smoke production.

For this aim, flame retardants and smoke suppressants are developed and utilized in PVC compounds. They can work in the gas or condensed phases and act physically or chemically. Refs. [17,22] give a detailed overview of mechanisms, types, and dosages.

1.4. Low-Smoke Acidity Compounds and Acid Scavengers at High Temperatures in the Condensed Phase

Low-smoke acidity PVC compounds have been developed to reduce the release of HCl in case of fire. In the low-smoke acidity compounds for cables, acid scavengers at high temperatures acting in the condensed phase are added to capture HCl [23,24]. The consequent reduction of HCl in the gas phase and metal chlorides in the condensed phase inhibits the fire performances of PVC compounds for cables: the consequence is the emission of more heat and smoke despite flame retardants and smoke suppressants added to the compounds.

The paper shows the impact of some acid scavengers at high temperatures on flame retardance and smoke emission of some PVC compounds for cables. Refs. [23,24] detail the main characteristics of the acid scavengers used in this paper, including dispersion properties and mechanism of action. This article compares the formulations with and without acid scavengers acting in the condensed phase. Ease of extinction has been measured according to ASTM D 2863 [25] (Limiting Oxygen Index, or LOI). Cone calorimetry has been used for determining heat release and smoke production according to ISO 5660-1 [26]. Micro combustion calorimetry (MCC) has been carried out according to ASTM D 7309 [27] to focus on the dynamic of the pyrolysis and combustion in the range of 250–750 °C. The presence of ATO in the PVC compound is entirely obliterated by the activity of potent acid scavengers that act by trapping HCl; that reflects in a lower LOI, higher fire growth rate (FIGRA), higher total heat release (THR), higher specific heat release (h_c), and higher specific heat of combustion of fuels gases ($h_{c\ gas}$). If a smoke suppressant is used in the presence of HCl scavengers, its action will be inhibited, causing a higher unexpected total smoke production (TSP).

The data indicate that low-smoke acidity PVC compounds will have fewer fire performances, and, therefore, finding other routes to get back the reaction to fire and smoke reduction becomes a task of extreme importance.

2. Materials and Methods

2.1. Materials

Table 1 shows the first set of formulations intending to show the interaction between acid scavengers at high temperatures in the condensed phase with a flame retardant acting in the gas phase, such as ATO. REA1 is the reference formulation without fillers, flame retardants, and smoke suppressants and represents the lower edge of performances in flame retardance and smoke production. REA2 comes from REA1 by adding 3 phr of ATO. It considers the effect of ATO without the impact of fillers capable of absorbing HCl interfering with the flame poisoning of ATO. REA3–5 focus on the effect of particle size of different grades of $CaCO_3$ on HCl absorption and its impact on flame retardancy

and smoke production. REA3 and REA4 contain ground milled calcium carbonate (GCC) with different particle sizes (Table 1), while REA5 contains ultrafine precipitated calcium carbonate (UPCC). REA6-8 focus on the different impacts on flame retardance by HCl scavengers having a different efficiency due to a different chemical nature: REA6 contains AS-6B, a potent acid scavenger at high temperatures in the condensed phase, REA7 contains an ineffective acid scavenger as MDH, and REA8 contains an inert acid scavenger such as ATH (see Section 4.1). The characteristics of those flame retardant fillers are well explained in Ref. [23]. REA9 shows the synergism between MDH and UPCC, described in the second part of this article [24]. That aims to highlight how they impact the HCl poisoning mechanism in the gas phase differently.

Table 2 formulations aim to show the impact of HCl scavengers on the performance of a potent flame retardant acting in the condensed phase. Reaguard B-FR/9211 is a commercial flame retardant and smoke suppressant produced by Reagens S.p.A. REAC0 contains exclusively 10 phr of Reaguard B-FR/9211, without flame retardant fillers. REAC1 contains ATH, not scavenging HCl, representing high flame retardancy and low smoke production levels. REAC2 contains MDH. It scavenges HCl, but it re-releases HCl again at 350–550 °C [28,29]. REAC4 contains UPCC, a potent acid scavenger that aims to verify if it interferes with the charring promoted by Reaguard B-FR/9211. REAC5 has GCC at the same phr as UPCC in REAC4.

Table 1. Inovyn 271 PC is a suspension PVC with a K value of 71 from Inovyn. DINP means Di Iso Nonyl Phthalate; Diplast N is the trade name of Polynt S.p.A. ESBO stands for Epoxidized Soy Bean Oil. Reaflex EP/6 is a Reagens trade name. The used antioxidant is Arenox A10, a Reagens trade name, which is Pentaerythritol tetrakis(3-(3,5-di-tert-butyl-4-hydroxyphenyl)propionate), CAS number 6683-19-8. COS stands for calcium organic stabilizer. RPK B-CV/3038 is a typical stabilizer for 70 °C cables produced by Reagens. Atomfor S and Hydrocarb 95 T are ground milled calcium carbonates, having a stearic acid coating and differing in medium value of particle size distribution (D50), 2.0 and 0.7 microns, respectively. Winnofil S is a UPCC having nanoscale mean particle size [30]. AS-6B is a potent acid scavenger in the condensed phase at high temperatures, produced by Reagens S.p.A, having a D50 of 2.0 microns. Ecopyren 3.5 is uncoated ground milled MDH produced by Europiren, with a D50 of 3.0 microns. Aluprem T GR 4 is a synthetic ATH from Tor Mineral, with a D50 of 2.5 microns (see Supplementary Materials).

Raw Materials	Trade Name	REA1 [phr]	REA2 [phr]	REA3 [phr]	REA4 [phr]	REA5 [phr]	REA6 [phr]	REA7 [phr]	REA8 [phr]	REA9 [phr]
PVC	Inovyn 271 PC	100	100	100	100	100	100	100	100	100
DINP	Diplast N	50	50	50	50	50	50	50	50	50
ESBO	Reaflex EP/6	2	2	2	2	2	2	2	2	2
Antioxidant	Arenox A10	0.1	0.1	0.1	0.1	0.1	0.1	0.1	0.1	0.1
COS	RPK B-CV/ 3038	5	5	5	5	5	5	5	5	5
Sb_2O_3	RI004	0	3	3	3	3	3	3	3	3
$CaCO_3$	Atomfor S	0	0	90	0	0	0	0	0	0
$CaCO_3$	Hydrocarb 95 T	0	0	0	90	0	0	0	0	0
UPCC	Winnofil S	0	0	0	0	90	0	0	0	90
HTAS 2	AS-6B	0	0	0	0	0	90	0	0	0
$Mg(OH)_2$	Ecopyren 3.5	0	0	0	0	0	0	90	0	30
$Al(OH)_3$	Aluprem T GR 4	0	0	0	0	0	0	0	90	0

The ingredient amounts in Tables 1 and 2 are expressed per hundred resin (phr). The formulations have been tested with the apparatuses in Table 3 and according to the test methods indicated in Table 4.

Table 2. Reaguard B-FR/9211 is a commercial flame retardant and smoke suppressant produced by Reagens S.p.A.

Raw Materials	Trade Name	REAC0 [phr]	REAC1 [phr]	REAC2 [phr]	REAC4 [phr]	REAC5 [phr]
PVC	Inovyn 271 PC	100	100	100	100	100
DINP	Diplast N	50	50	50	50	50
GCC	Atomfor S	0	30	30	0	90
$Al(OH)_3$	Aluprem TGR4	0	60	0	0	0
$Mg(OH)_2$	Ecopyren 3.5	0	0	60	0	0
UPCC	Winnofil S	0	0	0	90	0
COS	RPK B-CV/ 3038	3.0	3.0	3.0	3.0	3.0
Flame retardant	Reaguard B-FR/9211	10	10	10	10	10

Table 3. Main test apparatuses utilized.

Test Apparatus	Producer	Model	Additional Information
Calender	Battaggion	MCC/N150X300-E	Temperature 160 °C—Milling Time 3′
Halogen acid gas test apparatus	S.A. Associates	Standard model	Porcelain combustion boats
Multimeter for electric measurements	Mettler Toledo	S213 standard kit	
Conductivity electrode	Mettler Toledo	S213 standard kit	Reference thermocouple adjusting temperature fluctuations
pH electrode	ettler Toledo	S213 standard kit	Reference thermocouple adjusting temperature fluctuations
LOI test apparatus	FTT	Standard model	Test Specimen type IV; ASTM D 2863
Cone calorimeter	FTT	Dual cone calorimeter	ISO 5660-1. Heat flux 50 K.W./m^2, 1 or 3 mm test specimen thicknesses, with grid
Micro combustion calorimeter	FTT	Standard Model	Pyrolizer 1 °C/s, 750 °C, combustor 750 °C, method A of STM D 7309

Table 4. Tests for acidity, flame retardance, and smoke production assessments.

Technical Standard	Measurement	Temperature [°C]	Note
Internal method 3	Multimeter Smoke acidity	40 min to 800 °C +/−10 °C 20 min at 800°C +/−10 °C	DDW, pH, and conductivity. As EN 60754-2 with a heating regime of EN 60754-1
ASTM D 2863	LOI	23 °C	Test specimens type IV. Method B
ISO 5660-1	Time to ignition (TTI), (s) Time to flame out (TTFO) (s) Time to peak (TTP) (s) Peak of heat release rate (pHRR) (kW/m^2) Total heat release (THR) (MJ/m^2) Mass loss (%) Total smoke production (TSP) (m^2) Peak of smoke production rate (m^2/s) Yield of pyrolysis residue, (Yp) (g/g) Fire growth capacity (FGC) (J/g·K) Heat release capacity (η_c) (J/g·K)	755 °C	Sample thicknesses 1 mm and 3 mm, area 88.4 cm^2, sparkling source on
ASTM D 7309	Maximum specific heat release rate (Q_{max}) (J/g) Heat release temperature (T_{max}) (°C) Specific (total) heat release, h_c (J/g) Specific heat of combustions of fuel gases, $h_{c\ gas}$ (J/g)	750 °C combustor 1 °C/min to 750 °C pyrolizer	

Internal method 3, described in Table 4, uses the following materials: double deionized water (DDW) is internally produced by an ion exchange deionizer. The pH of DDW must be between 5.50 and 7.50, and the conductivity must be less than 0.5 µS/mm. Buffer and conductivity standard solutions come from VWR international (pH: 2.00, 4.01, 7.00, 10.00; conductivity: 2.0, 8.4, 14.7, 141.3 µS/mm).

2.2. Test Apparatuses

Table 3 describes the utilized test apparatuses.

2.3. Sample Preparation

The formulations in Tables 1 and 2 were prepared in a turbo mixer producing the dry blends, then processed in the laboratory calender. The foils produced test specimens for internal method 3 and MCC and were shaped in a hydraulic press in plaques with 1.0 and 3.0 mm thicknesses for the cone calorimeter and 3.0 mm plaques for LOI. In Appendix A, Figures A1 and A2 give a schematic diagram with a more detailed description of the sample preparation.

2.4. Internal Tests and International Technical Standards Used

Table 4 shows the technical standards, internal methods, and the main utilized conditions.

Internal method 3 is carried out as EN 60754-2 [31], using the heating regime of EN 60754-1 [32] and following the indications and suggestions highlighted in Ref. [23]. The sample, introduced in the tube furnace at room temperature, was heated for 40 min to 800 °C and then kept at 800 °C for 20 min. The smoke was collected in two bubblers containing DDW. The water from the bubbling devices and the washing procedures was collected in a 1 L volumetric flask filled to the mark. pH and conductivity were measured, and two replicates gave mean value, standard deviation (SD), and coefficient of variation (CV).

LOI was measured following the procedure described in ASTM D 2863 [25], as indicated in paragraph 12, procedure B. Three replicates gave mean and SD. ISO 5660-1 [26] was performed using two replicates, calculating mean values and SD at an incident heat flux of 50 kW/m^2, corresponding to a temperature of 755 °C. According to the standard, the test specimens had dimensions of 100 mm × 100 mm with thicknesses of 1 or 3 mm and an effective exposed area of 88.4 cm^2. FIGRA was calculated, as described in EN 13823 [33], as the maximum multiplied per 1000 of the function HRR/t (t), excluding data corresponding to THR (t) < 0.2 MJ and HRR (t) < 3 kW/m^2. ASTM 7309 [27] was performed on three replicates to calculate the mean and SD, according to method A. Fluxes of 80 mL/min of N_2 in the pyrolizer and 20 mL/min of O_2 in the combustor were set. The temperature of the combustor was adjusted to 750 °C +/− 1 °C, and in the pyrolizer, a heating regime of 1 °C/min was chosen up to 750 °C. The sample's weight was determined, evaluating the oxygen consumption of a trial test. The drop must stay between 20–13% and 20–7%.

In Appendix A, Figure A2 gives a schematic diagram of the conditions used in the test methods.

3. Results

The results of the formulations in Tables 1 and 2 are summarized as follows: Tables 5 and 6 show the pH and conductivity, Tables 7 and 8 report LOI, Tables 9 and 10 summarize cone calorimetry data, and Tables 11 and 12 display MCC measurements.

Table 5. pH and conductivity of the compounds in Table 1 are shown. Internal method 3 has been carried out. The mean values and CV are reported. CVs are below 5%.

Formulation	REA1	REA2	REA3	REA4	REA5	REA6	REA7	REA8	REA9
pH	2.20	2.30	2.60	2.90	3.20	4.20	2.50	2.40	3.40
CV_{pH}	<5.0%	<5.0%	<5.0%	<5.0%	<5.0%	<5.0%	<5.0%	<5.0%	<5.0%
Conductivity (µS/mm)	359.7	328.5	105.7	70.1	31.1	3.8	180.7	205.2	11.8
CV_c	<5.0%	<5.0%	<5.0%	<5.0%	<5.0%	<5.0%	<5.0%	<5.0%	<5.0%

Table 6. pH and conductivity of the compounds in Table 2 are shown. Internal method 3 has been carried out. The mean values, coefficient of variation, and standard deviations are reported.

Formulation	REAC0	REAC1	REAC2	REAC4	REAC5
pH	1.95	2.65	2.74	3.30	2.62
CV_{pH}	<5.0%	<5.0%	<5.0%	<5.0%	<5.0%
Conductivity (µS/mm)	462.1	92.8	76.0	25.1	117.3
CV_c	<5.0%	<5.0%	<5.0%	<5.0%	<5.0%

Table 7. LOIs of the compounds in Table 1 are shown. The mean values, coefficient of variation, and standard deviations are reported.

Formulation	REA1	REA2	REA3	REA4	REA5	REA6	REA7	REA8	REA9
LOI (O_2%)	24.0	29.0	28.0	27.3	22.0	23.0	34.7	34.0	24.0
SD	1.0	0.0	0.0	0.6	0.0	0.6	0.6	0.0	1.0

Table 8. LOIs of the compounds in Table 2 are shown. The mean values, coefficient of variation, and standard deviations are reported.

Formulation	REAC0	REAC1	REAC2	REAC4	REAC5
LOI (O_2%)	25.0	29.3	28.0	21.0	25.0
SD	0.0	1.5	1.0	0.0	0.0

Table 9. Cone calorimetry measurements of the compounds in Table 1 are shown. The mean values, coefficient of variation, and standard deviations are reported. Results are referred to as 3 mm plaques.

Formulation	REA1	REA2	REA3	REA4	REA5	REA6	REA7	REA8	REA9
peak HRR (kW/m^2)	337.5	252.4	192.1	213.0	331.6	394.3	167.7	105.0	254.8
SD	31.0	6.4	9.5	3.3	5.6	13.0	7.7	2.1	10.7
THR (MJ/m^2)	55.0	49.1	43.8	40.0	58.8	45.5	39.4	40.0	53.5
SD	0.7	0.9	1.7	2.0	1.5	1.3	1.9	1.4	3.3
FIGRA (W/s)	4187	3098	2549	3224	4073	5110	1563	1597	3365
SD	147	129	458	83	594	503	146	194	255
TSP (m^2)	28.3	28.1	16.5	17.8	13.8	15.3	10.1	9.6	11.4
SD	0.6	1.3	1.0	1.2	0.5	0.3	1.5	1.8	0.5

Table 10. Cone calorimetry measurements of the compounds in Table 2 are shown. The mean values, coefficient of variation, and standard deviations are reported. Results are referred to as 1 mm plaques.

Formulation	REAC0	REAC1	REAC2	REAC4	REAC5
peak HRR (kW/m^2)	270.4	128.4	200.5	292.6	198.8
SD	33.2	0.5	11.4	1.1	7.4
THR (MJ/m^2)	18.0	20.2	25.4	29.7	23.6
SD	0.5	1.6	2.2	0.1	3.3
FIGRA (W/s)	6239	2616	3986	6035	4316
SD	49	215	402	220	542
TSP (m^2)	6.4	3.9	4.6	6.6	5.1
SD	0.6	0.5	0.1	0.4	0.6

Table 11. MCC measurements of the compounds in Table 1 are shown. The mean values and standard deviations are reported. FGC is the fire growth capacity, HRR means heat release rate, PR is pyrolysis residue, Q max is the maximum of specific HRR, T max is the heat release temperature, h_c is the specific (total) heat release, Y_p the yield of pyrolysis residue, h_c gas is the specific heat of combustion of fuels gases, and Stg means stage.

Formulation	REA1	REA2	REA3	REA4	REA5	REA6	REA7	REA8	REA9
FGC (J/g·K)	156.95	141.42	88.90	90.83	104.72	100.51	75.81	102.43	92.83
SD	5.52	2.41	0.70	0.19	0.23	3.05	2.73	1.63	1.20
η_c (J/g·K)	324.10	326.11	330.20	333.33	338.65	322.50	323.30	321.01	333.03
SD	24.08	8.77	4.94	0.97	5.30	13.23	13.41	7.75	6.71
Qmax (J/g) stg 1	202.00	197.79	135.26	152.50	162.78	144.00	109.86	136.03	147.31
SD	4.78	4.65	0.65	3.33	5.94	4.51	2.13	7.80	2.19
Tmax (°C) stg 1	324.1	326.1	330.2	333.3	338.6	322.5	323.3	321.0	333.0
SD	0.81	1.20	0.30	1.60	0.80	6.20	2.30	1.00	0.20
Qmax (J/g) stg 2	101.61	96.93	51.36	51.37	57.34	51.97	52.62	48.77	59.49
SD	5.69	3.90	0.50	0.54	0.30	1.89	0.38	0.08	1.29
Tmax (°C) stg 2	491.8	493.0	483.5	475.7	480.5	500.6	486.8	478.0	478.8
SD	0.99	1.10	0.16	1.00	0.30	1.70	0.40	2.20	0.90
h_c (J/g) total	17.16	15.42	9.93	10.23	11.76	11.33	9.15	10.38	10.38
SD	0.19	0.17	0.12	0.06	0.03	0.16	0.10	0.09	0.08
h_c (J/g) stg 1	10.31	9.00	5.86	6.31	7.32	6.64	4.74	6.56	6.00
SD	0.18	0.17	0.08	0.06	0.04	0.21	0.09	0.17	0.06
h_c (J/g) stg 2	6.85	6.42	4.07	3.92	4.44	4.69	4.41	3.83	4.38
SD	0.20	0.17	0.16	0.05	0.02	0.11	0.11	0.07	0.10
Yp (g/g)	0.08	0.13	0.35	0.40	0.43	0.48	0.34	0.33	0.46
SD	0.03	0.01	0.02	0.02	0.00	0.02	0.01	0.02	0.02
$h_{c\ gas}$ (J/g) total	18.71	17.84	15.30	16.94	20.65	21.95	13.92	15.73	19.08
SD	0.12	0.27	0.35	0.54	0.11	1.11	0.42	0.32	0.60
$h_{c\ gas}$ (J/g) stg 1	11.24	10.41	8.95	10.45	12.86	12.86	7.22	9.94	11.03
SD	0.10	0.11	0.26	0.35	0.08	0.63	0.20	0.45	0.43
$h_{c\ gas}$ (J/g) stg 2	7.48	7.43	6.35	6.50	7.80	9.09	6.70	5.82	8.05
SD	0.02	0.16	0.09	0.19	0.03	0.48	0.22	0.19	0.17

Table 12. MCC measurements of the compounds in Table 2 are shown. The mean values and standard deviations are reported. FGC is the fire growth capacity, HRR means heat release rate, PR is pyrolysis residue, Q max is the maximum of specific HRR, T max is the heat release temperature, h_c is the specific (total) heat release, Y_p the yield of pyrolysis residue, h_c gas is the specific heat of combustion of fuels gases, and Stg means stage.

Formulation	REAC0	REAC1	REAC2	REAC4	REAC5
FGC (J/g·K)	102.68	83.66	79.99	93.90	76.69
SD	6.25	0.72	1.30	1.67	0.82
η_c (J/g·K)	366.66	212.13	259.66	229.07	287.92
SD	13.40	4.71	4.92	8.83	21.21
Qmax (J/g) stg 1	277.68	123.38	196.29	141.61	166.51
SD	12.84	6.25	8.19	6.65	2.56
Tmax (°C) stg 1	303.4	326.5	314.8	334.1	325.0
SD	0.1	1.7	0.8	1.4	0.8
Qmax (J/g) stg 2	62.13	44.64	51.71	52.57	48.14
SD	3.50	1.00	1.05	1.20	1.25
Tmax (°C) stg 2	481.6	481.2	485.2	482.8	485.9
SD	1.2	2.1	0.8	1.0	2.0
h_c (J/g) total	12.25	9.97	9.60	11.32	9.41
SD	0.27	0.12	0.16	0.15	0.10
h_c (J/g) stg 1	8.06	6.63	5.81	7.34	6.15
SD	0.37	0.13	0.11	0.10	0.03
h_c (J/g) stg 2	4.19	3.33	3.80	3.98	3.27
SD	0.17	0.07	0.10	0.07	0.16
Yp (g/g)	0.18	0.36	0.43	0.44	0.39
SD	0.03	0.01	0.05	0.05	0.03
$h_{c\ gas}$ (J/g) total	15.54	15.74	16.55	20.94	15.70
SD	0.14	0.10	1.45	1.13	0.36
$h_{c\ gas}$ (J/g) stg 1	10.17	10.44	9.81	13.55	10.19
SD	0.14	0.09	1.25	0.86	0.55
$h_{c\ gas}$ (J/g) stg 2	5.36	5.29	6.74	7.38	5.50
SD	0.13	0.07	0.58	0.41	0.16

4. Discussion

4.1. Description of the Impact of Acid Scavengers on pH and Conductivity

Table 5 reports pH and conductivity according to internal method 3 for samples REA1–9, containing ATO as a flame retardant in the gas phase. Internal method 3 is more appropriate than EN 60754-2 in evaluating the smoke acidity in this research due to a heating regime that allows the acid scavenger to interact better with HCl [34]. REA1 and REA2 show the highest smoke acidity (low pH and high conductivity values) since they do not contain any acid scavenger at high temperatures in the condensed phase and have a higher PVC percentage than REA3–9. REA7 and REA8 have ineffective and inert acid scavengers, MDH and ATH; indeed, they show high acidity values because ATH does not react with HCl, while MDH scavenges HCl, but it then decomposes between 350 °C and 550 °C, thus re-releasing HCl [24,28,29]. Both samples show higher acidity than REA3, the formulation with GCC. REA3–5 contain different types of calcium carbonate with different particle size. Atomfor S has a mean particle size of around 2 microns, while Hydrocarb 95 T reaches low values down to 0.7 microns. Winnofil S is a coated UPCC with a mean particle size in nanoscale size [30]. REA6 and 9 give the lowest smoke acidity values due to powerful acid scavengers (ASB-6, REA6) and the synergistic couple MDH/UPCC in REA9 [24].

Table 6 shows pH and conductivity according to internal method 3 for samples REAC0-C5, containing REAGUARD B-FR/9211 as a flame retardant acting in the condensed phase. REAC0 without fillers and acid scavengers displays the highest acidity. REAC5, REAC1, and REAC2 with GCC, ATH, and MDH, respectively, follow in this sequence. REAC4 with

UPCC, as expected, reaches the lowest acidity values. The comparison between REAC4 and REAC5 again shows how profoundly the particle size impacts the smoke acidity.

4.2. Effect of Acid Scavenging on LOI

HCl sequestration impacts the LOI values of the formulations in Table 1, containing ATO acting in the gas phase (Table 7), and the formulations in Table 2 with Reaguard B-FR/9211 acting in the condensed phase (Table 8).

REA1, without a flame retardant, shows 24.0 $\%O_2$ LOI. REA2 containing 3 phr of ATO, gains 5 LOI points reaching 29.0 $\%O_2$. The addition of 90 phr of Atomfor S in REA3 depresses LOI slightly (28.0 $\%O_2$), but the impact becomes more evident as the particle size of $CaCO_3$ decreases and the HCl scavenging efficiency increases: REA3 with 2 microns $CaCO_3$ shows 28.0 $\%O_2$ comparable with REA4 (27.3 $\%O_2$) having 0.7 microns, while REA5 with UPCC has LOI even lower than REA1 without ATO (22.0 $\%O_2$). Using a powerful single-step HCl scavenger such as AS-6B (REA6) or multiple-step such as the couple Winnofil S and MDH (REA9), the trend is the same: REA6 LOI goes down to 23.0 $\%O_2$ and REA9 to 24.0 $\%O_2$. In both formulations containing Winnofil S and AS-6B, the action of ATO is inhibited by HCl scavenging in the gas phase, and LOI values collapse. REA9 has a slightly higher LOI (24.0 $\%O_2$) due to MDH's different mechanism of action as a flame retardant: it acts as a heat sink through an endothermic decomposition, dilutes the flame's fuels, and creates a barrier of MgO in the condensed phase. REA7 and REA8, containing ATH and MDH, boost LOI due to their specific mechanisms as flame retardants [17] and because they do not scavenge HCl. Figure 1 summarizes the data.

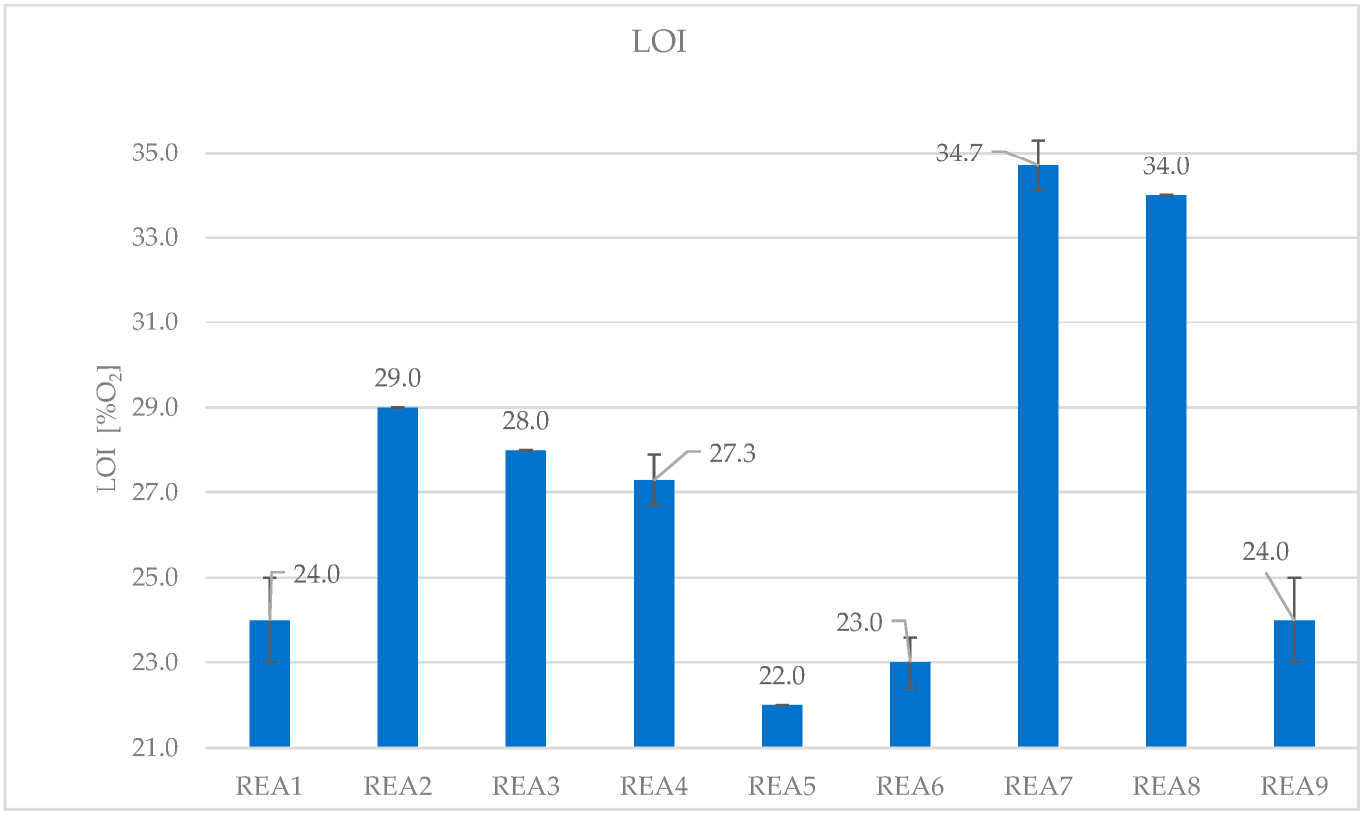

Figure 1. LOI of the formulations in Table 1, REA1–REA9.

HCl scavenging has the same impact when the flame retardant acts in the condensed phase. REAC0 contains only Reaguard B-FR/9211. LOI increases slightly compared to REA1 without a flame retardant (25.0 $\%O_2$ vs. 24.0 $\%O_2$). The introduction of ATH and MDH increases the LOI in REAC1 and REAC2 (29.3 $\%O_2$ and 28.0 $\%O_2$, respectively). As expected, both flame retardant fillers work synergistically with Reaguard B-FR/9211. When

UPCC is in the formulation at 90 phr (REAC4), its scavenging action depresses LOI down to 21.0 $\%O_2$, which is (even) lower than the formulation without flame retardants (REA1). The formulation with GCC, REAC5, shows the same LOI as REAC0. Figure 2 shows the summarized data.

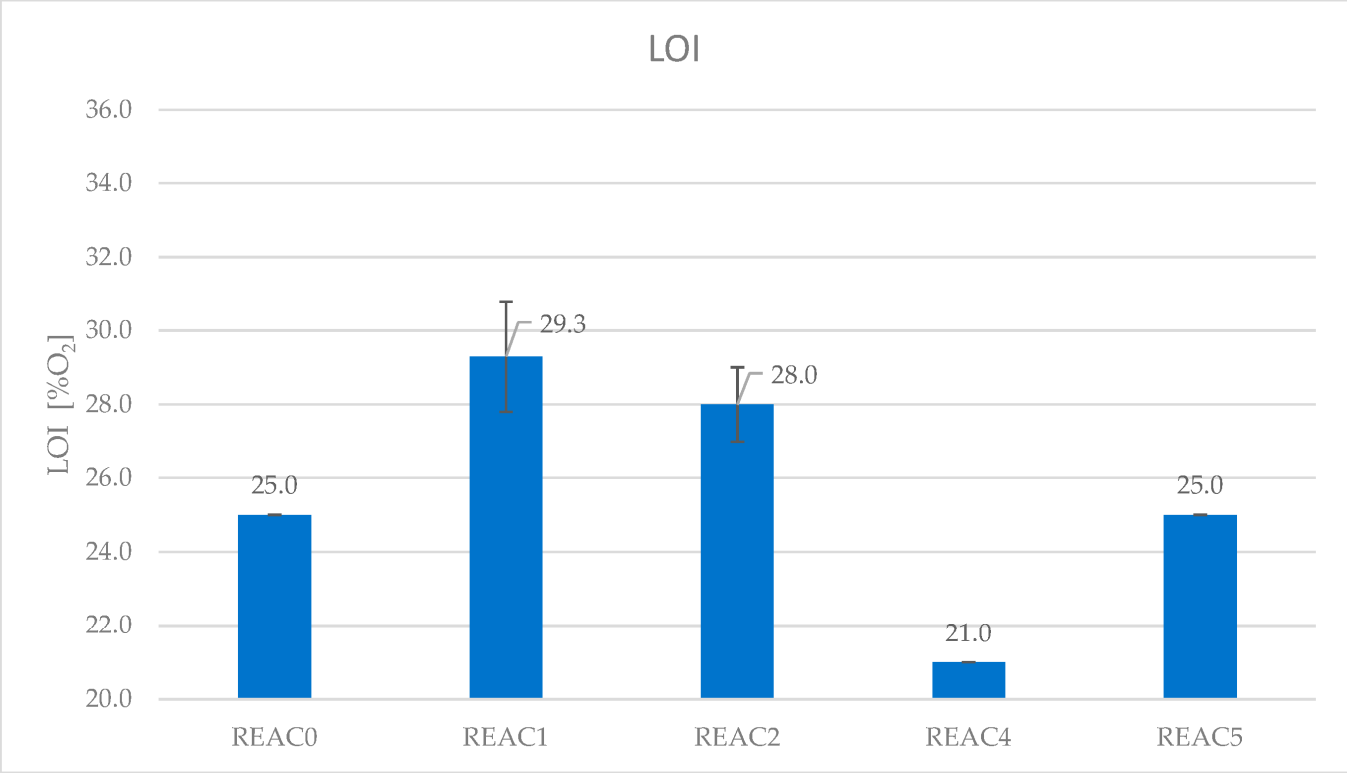

Figure 2. LOI of the formulations in Table 2, REAC0–REAC9.

Finally, the HCl sequestration of a potent acid scavenger depresses the ease of extinction of the formulation imparted by flame retardants acting both in the gas and condensed phase.

4.3. Effect of Acid Scavenging on Heat Release Rate and Smoke Production Measured in Cone Calorimetry

In fire science, the HRR is among the most critical parameter to be evaluated since it can parametrize the "intensity of the fire" [35,36].

The presence of acid scavengers strongly influences the HRR and THR of the formulations reported in Table 1 containing ATO as a flame retardant, as reported in Table 9. pHRR represents the maximum peak of the HRR (t) curve: the higher the peak, the lower the fire performance. Figure 3 clearly shows how acid scavengers at high temperatures affect this measure. REA1 is a formulation that contains neither filler nor ATO and can be considered the lower edge in fire performances. Its peak reached 337.5 kW/m^2, and with the addition of ATO In the formulation REA2, the peak dropped severely to 252.4 kW/m^2. REA3, containing 90 phr of GCC in addition to ATO and, hence, less incombustible material, shows an even lower value of pHRR than REA2. REA3, REA4, and REA5 contain, respectively, GCC, a finer GCC, and UPCC. The finer the particle size, the higher the peak (192.1 kW/m^2, 213.0 kW/m^2, and 331.6 kW/m^2, respectively). REA6, with a powerful acid scavenger, shows a pHRR much higher than the REA1 without flame retardants. REA7 and REA8 contain ineffective and inert acid scavengers, MDH and ATH. Here, HCl is released almost stoichiometrically and stops the action of the radicals feeding the flame. Therefore, because of their extremely low efficiencies in HCl scavenging and their flame retardant action, they show the lowest pHRR values (167.7 kW/m^2 and 105.0 kW/m^2). REA9 contains MDH

and UPCC in the correct ratio for working synergistically in HCl scavenging [23,24]. REA9 shows better fire performances because it contains more incombustible filler (REA9, 130 phr vs. REA6, 90 phr), and one of them, MDH, is capable of working as a flame retardant even in low-acidity conditions. Indeed, REA9 yields a minor smoke acidity (Table 5), but pHRR is lower than REA1, showing that the flame retardancy imparted by MDH is not inhibited by HCl sequestration.

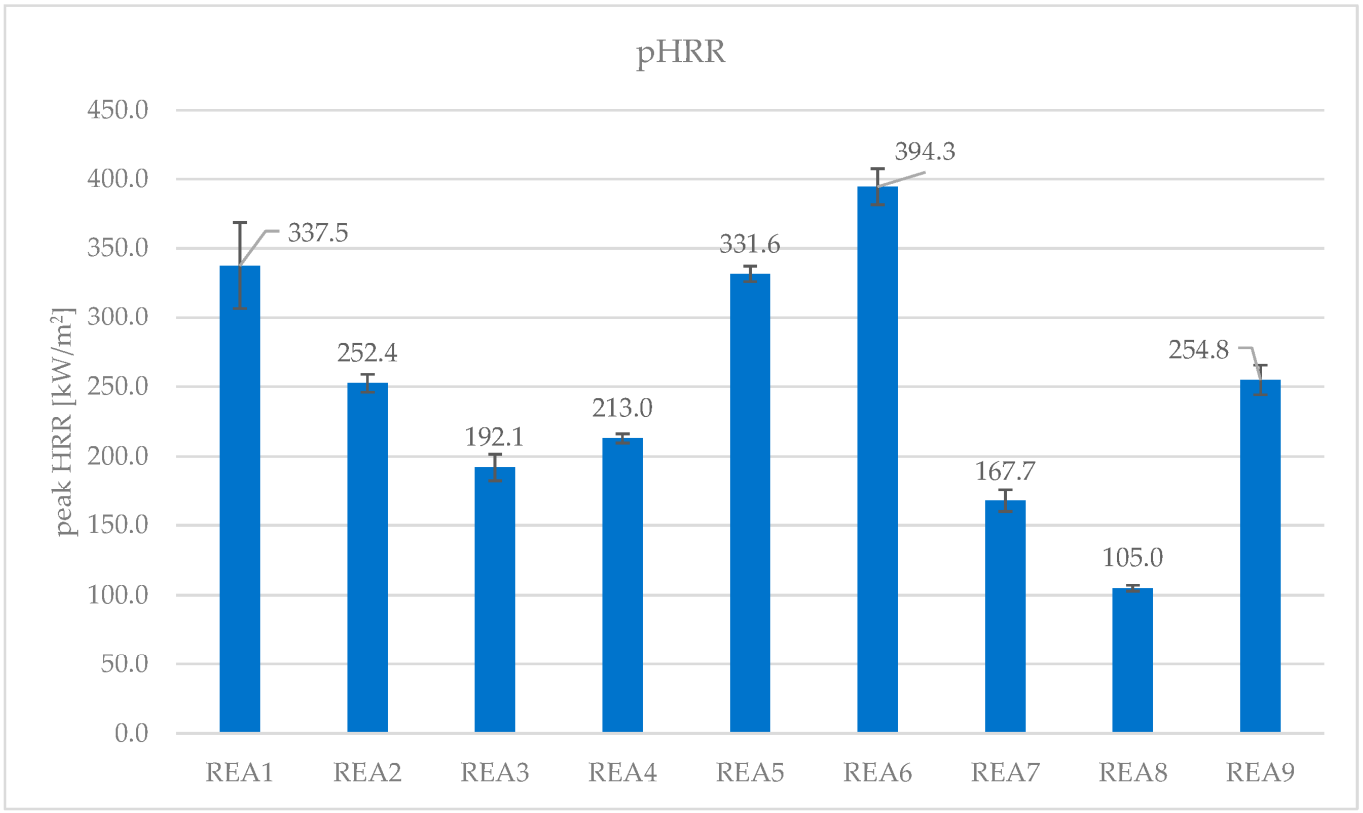

Figure 3. pHRR of the formulations in Table 1, REA1–REA9.

FIGRA is the ratio of the maximum of derivate of the function HRR (t) vs. the time required to reach it; such an index represents the maximum growth rate of the heat release rate and is helpful in ranking the material in terms of potential fire safety. Consequently, the higher the FIGRA, the lower the fire performance of the article. The measurements in Table 9 and Figure 4 indicate the reciprocity between the loss of flame retardance and the HCl availability in the gas phase. REA6, containing a potent acid scavenger, gives a FIGRA much higher than REA1, and the effect of $CaCO_3$ with different particle sizes is highlighted in REA3–REA5, where UPCC in REA5 shows the highest FIGRA in the group. REA7 and REA8, the worst in terms of smoke acidity, provide the best FIGRA of the formulations in Table 1. Again, REA9 compensates for the lack of flame retardance (in REA5) thanks to the presence of MDH and more incombustible flame retardant fillers and acid scavengers.

Total heat release (THR), in Table 9, is the area below the HRR (t) curve and accounts for the heat release in 600 s of the test in the cone calorimetry. Data are summarized in Figures 5 and 6.

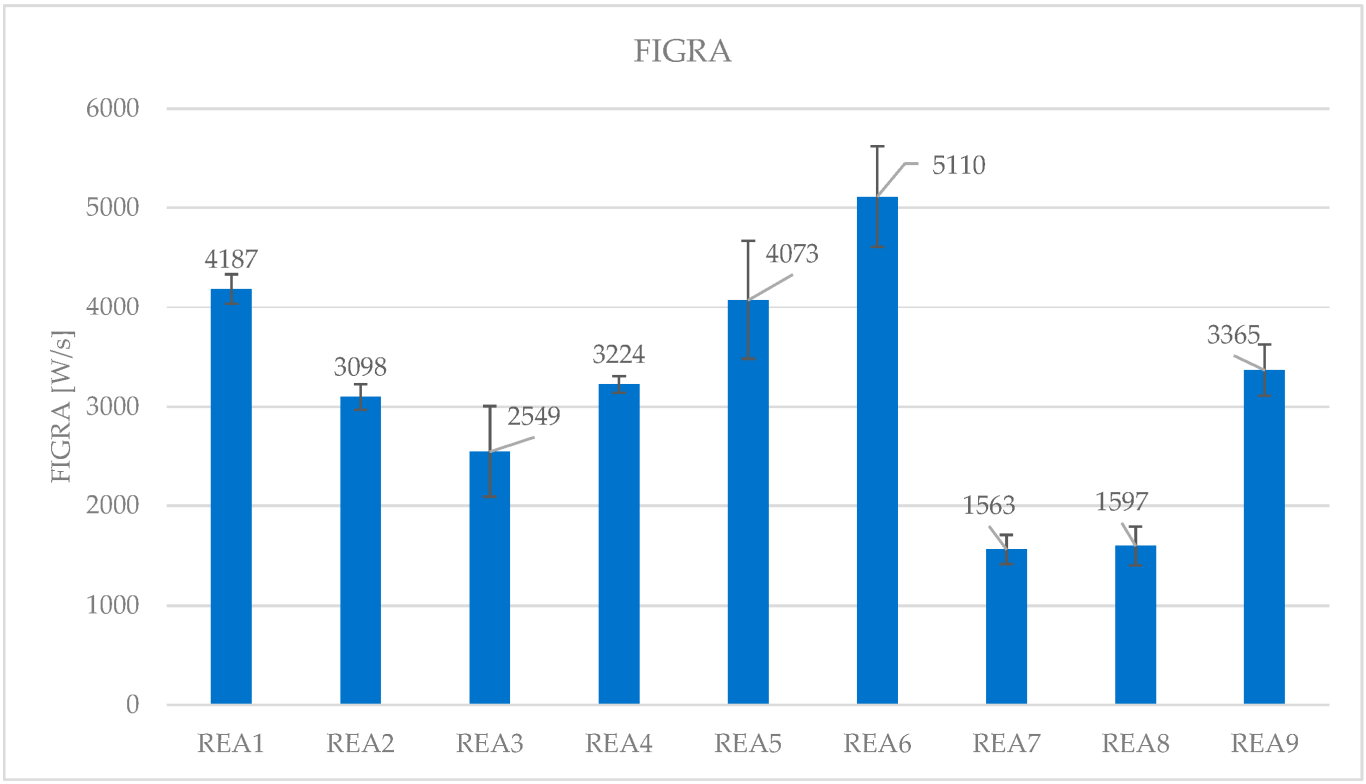

Figure 4. FIGRA of the formulations in Table 1, REA1–REA9.

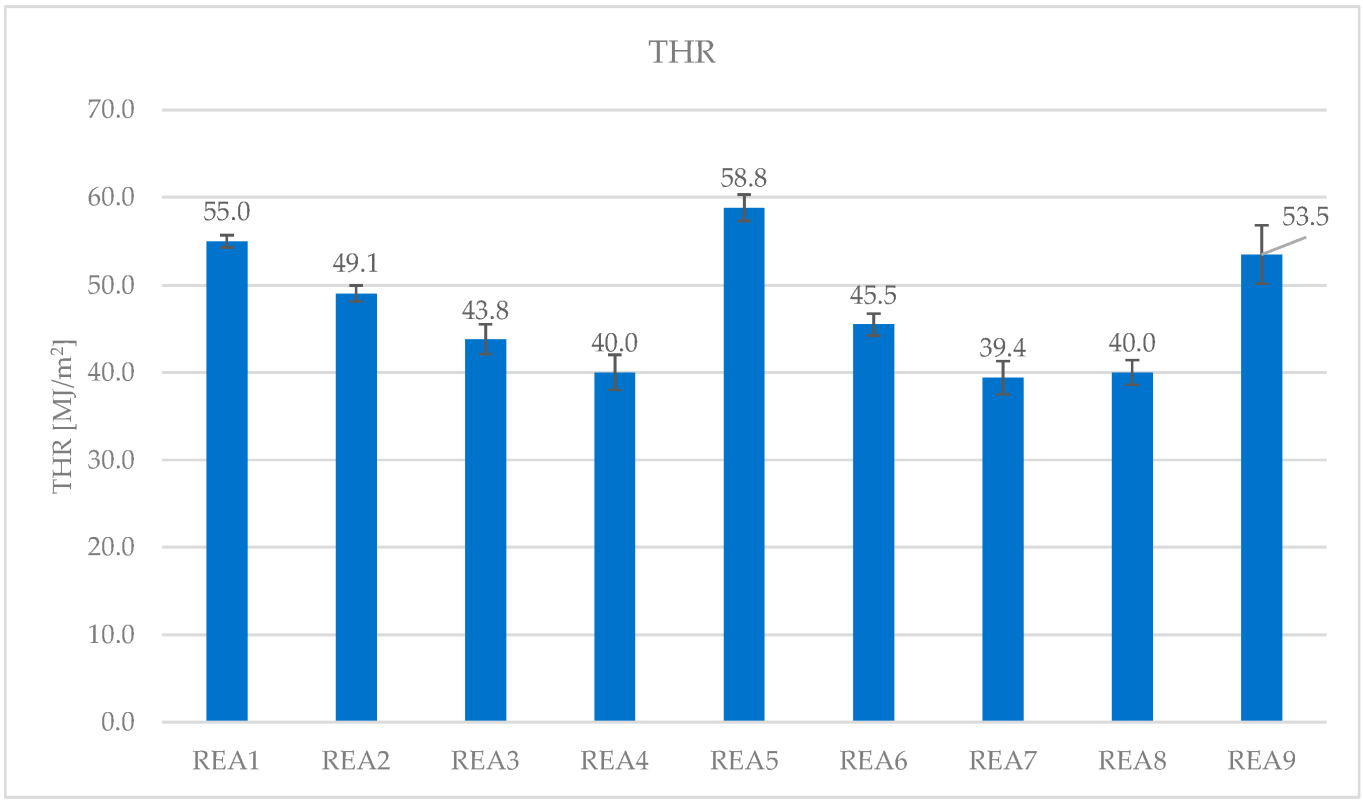

Figure 5. THR of the formulations in Table 1, REA1–REA9.

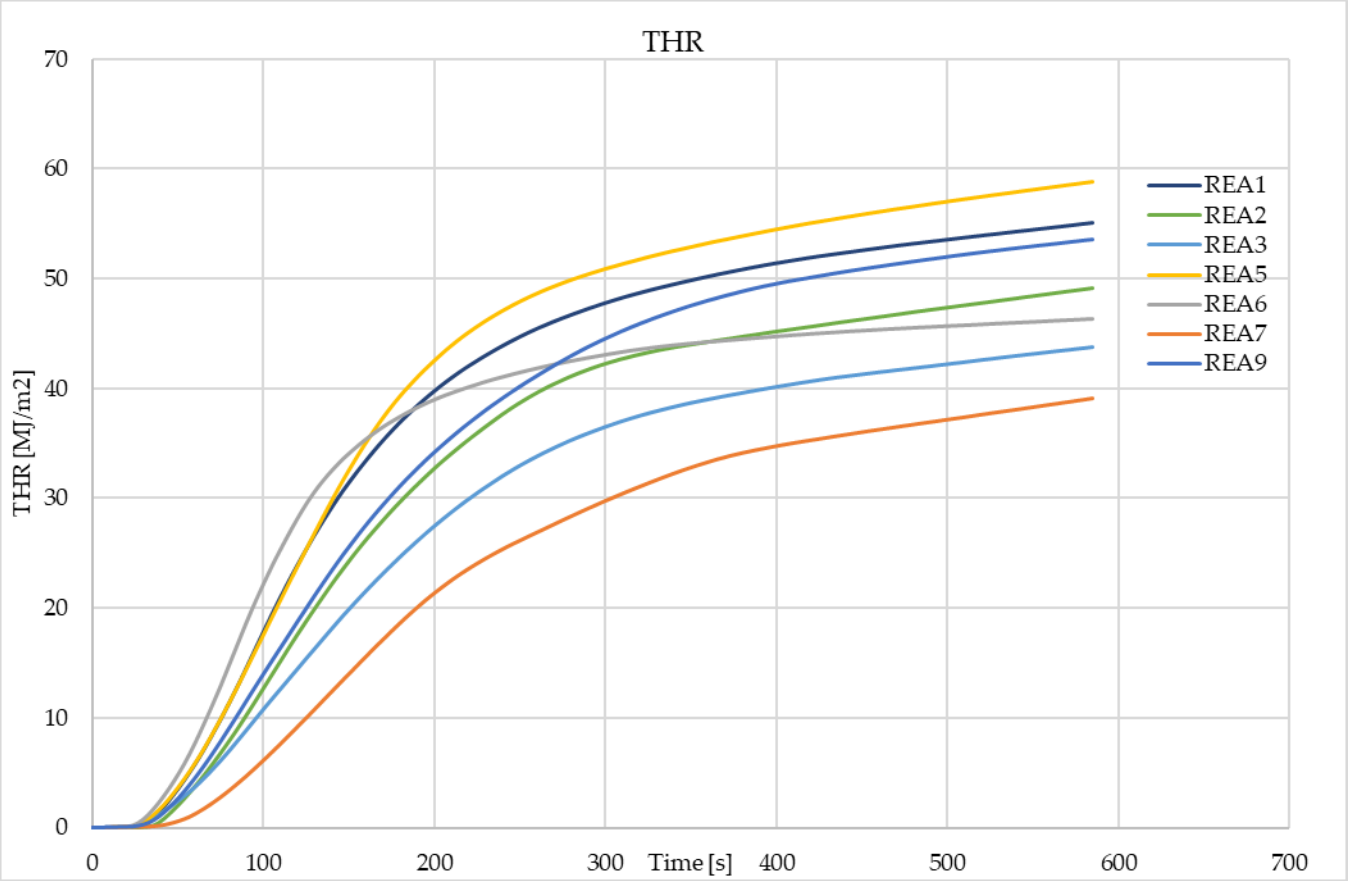

Figure 6. THR (t) of the formulations in Table 1, REA1–REA9.

HCl scavenging seems to have a substantial effect on speeding the velocity at which the heat is released. It also contributes to the intensity of the peak of HRR (t) but to a lesser extent on THR. REA5 shows the highest THR value (58.8 MJ/m^2). REA9 and REA6 follow with peaks higher than REA3 but lower than REA1 and REA2 (Table 9, Figures 5 and 6). In the formulations REA1–9, the flame retardant mechanism in the gas phase is promoted by ATO. In the first stage of the decomposition/combustion, the negative contribution to the flame retardancy by HCl sequestration is given. It is unclear why REA5 shows higher THR values than REA6 (Table 9, Figures 5 and 6), despite yielding more smoke acidity. REA6 seems to release heat faster, but in the end, its THR is lower than REA5. That is probably due to a different scavenging mechanism. REA6 scavenges HCl faster and more efficiently than REA5, reflecting a higher pHRR (Figure 7). However, the reason why REA6 THR is lower than REA5 THR is unknown and difficult to understand with the current measurements and data. However, understanding these differences is out of this paper's scope but is crucial in designing flame retardants, smoke suppressants, and acid scavengers working well together.

In cone calorimetry, a dynamic measure of smoke production is possible. The smoke production rate, SPR (t), is measured, and the area below the curve represents the total smoke production, TSP. Smoke production measures are critical in fire safety because smoke can hamper people involved in fire from escaping unharmed or being rescued by firefighters.

TSP values of the formulations of Table 1 (reported in Figure 8) show that REA1 and REA2 have the worst smoke production performance in the series, with comparable results (REA1 28.3 m^2 and REA2 28.1 m^2, respectively). The analysis of data of the remaining formulations is not easily parameterized. There is no clear correlation between HCl sequestration and smoke, but it should be highlighted that the formulations in Table 1 contain

ATO, which works in the gas phase; therefore, it is a system where smoke production is not inhibited by the presence of substances acting in the condensed phase. It appears that smoke production is just inversely proportional to the content of the fraction burning in the matrix since REA3–9 show fewer TSP than REA1 and REA2. REA7 and REA8 give the lowest values of smoke, probably due to the action of ATH and MDH on smoke production, as Ref. [18] reports.

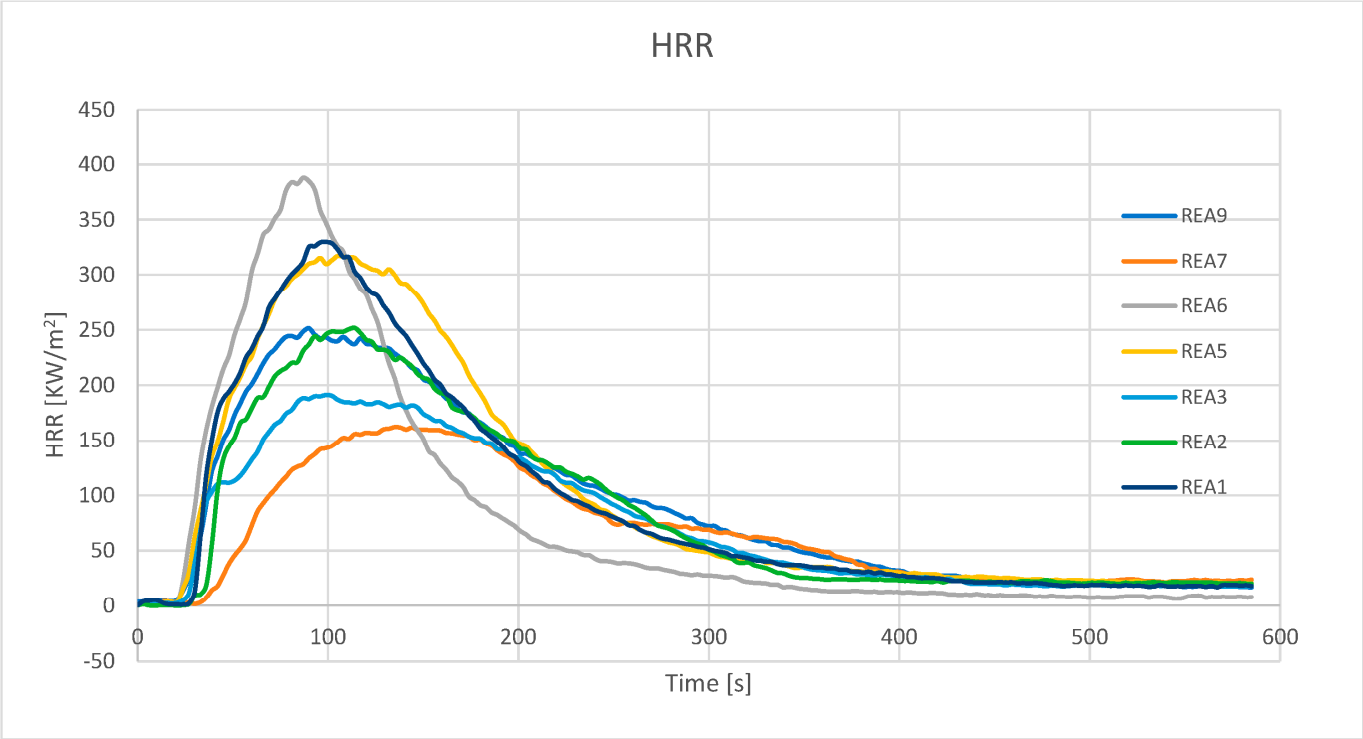

Figure 7. HRR (t) of the formulations in Table 1, REA1–REA9.

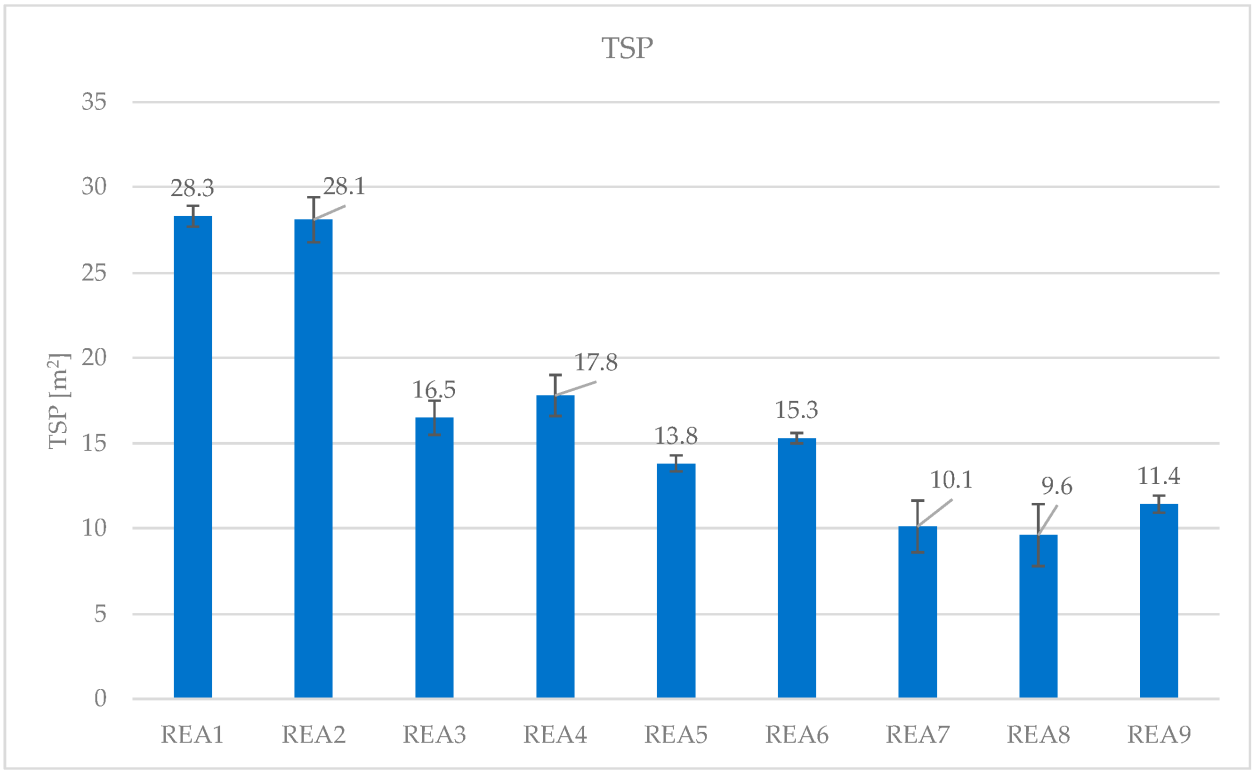

Figure 8. TSP of the formulation REA1–REA9.

In the formulations of Table 2, where the flame retardant acts in the condensed phase, the cone calorimeter measurements (Table 10, Figures 9–15) indicate the interference of HCl sequestration on cross-linking of actual Lewis acid: they clearly show the increase of heat release when HCl scavengers are used.

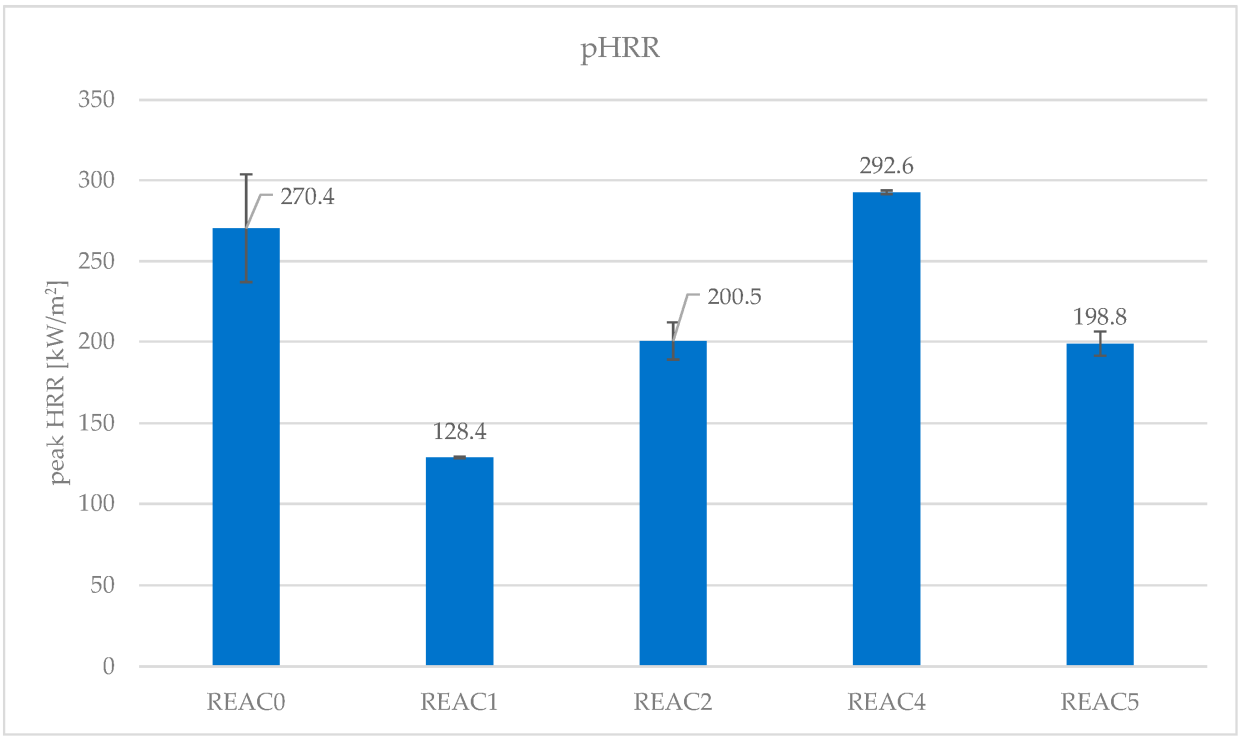

Figure 9. pHRR of the formulations REAC0–5.

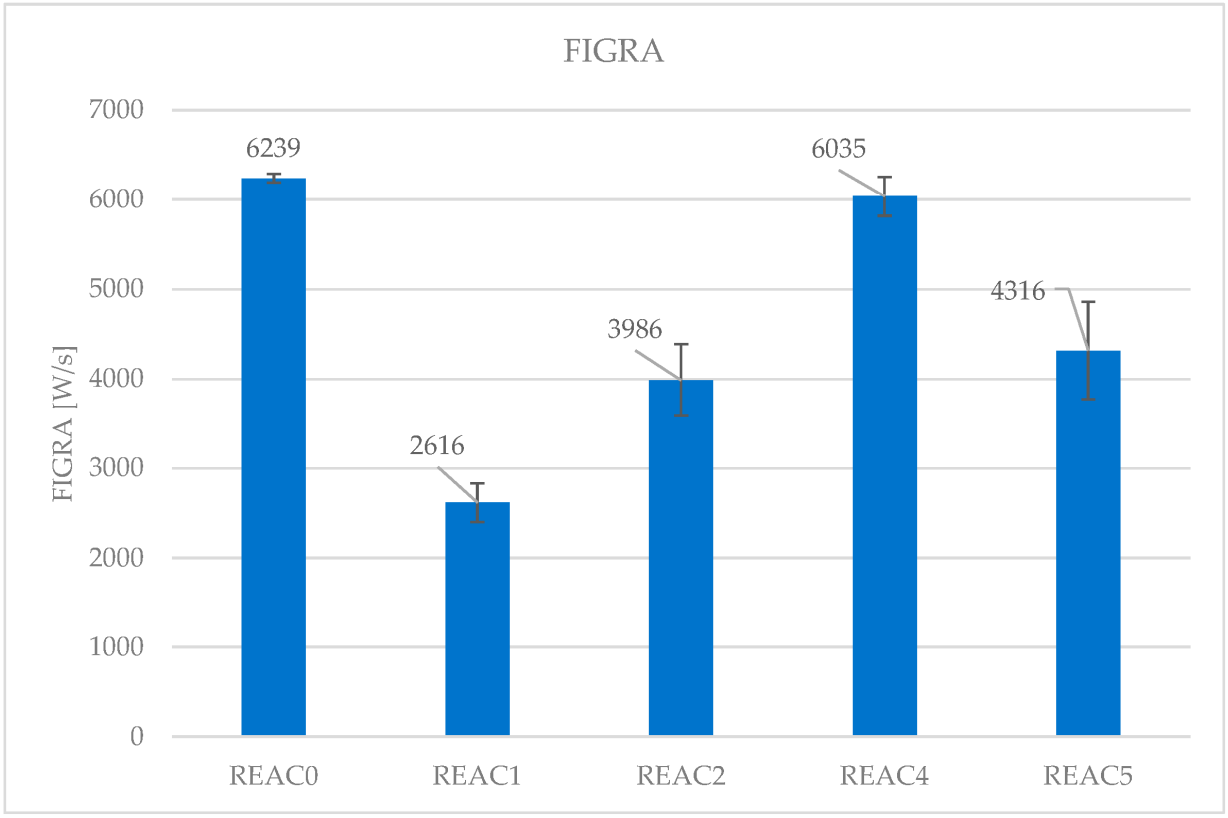

Figure 10. FIGRA of the formulations REAC0–5.

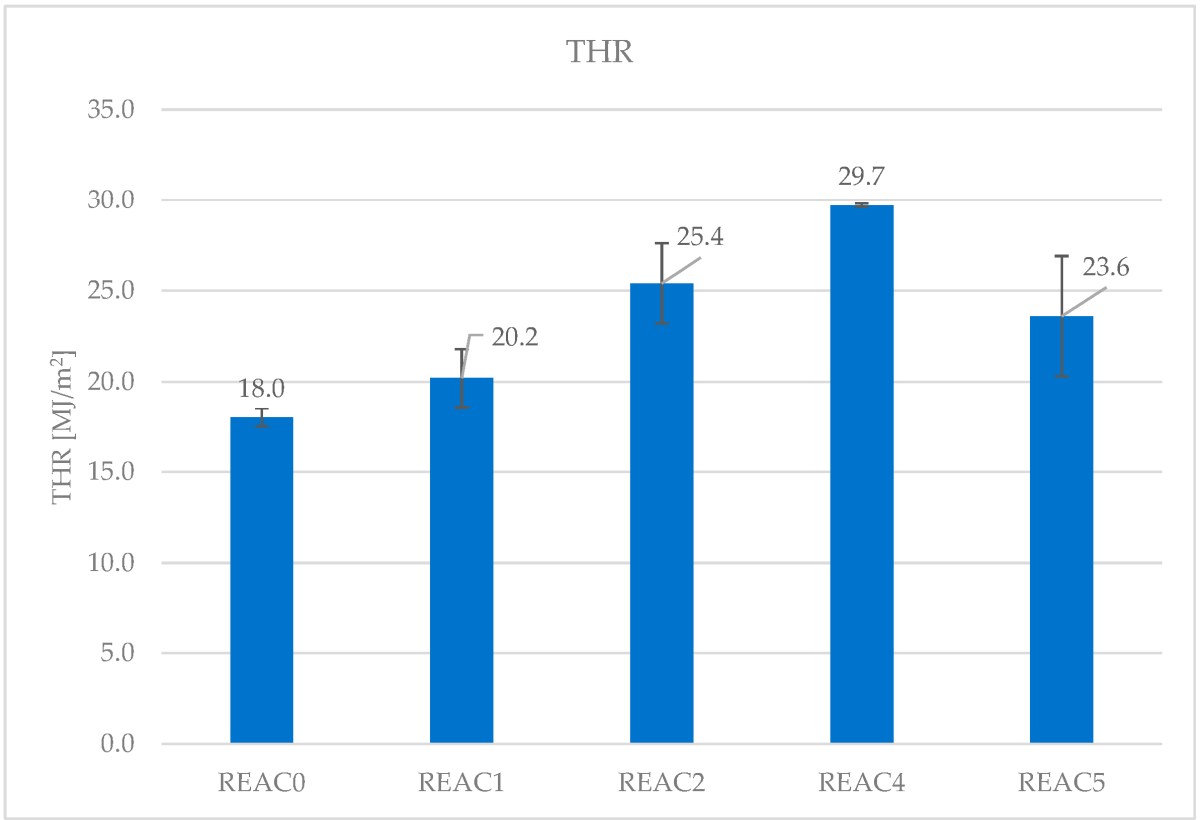

Figure 11. THR of the formulations REAC0–5.

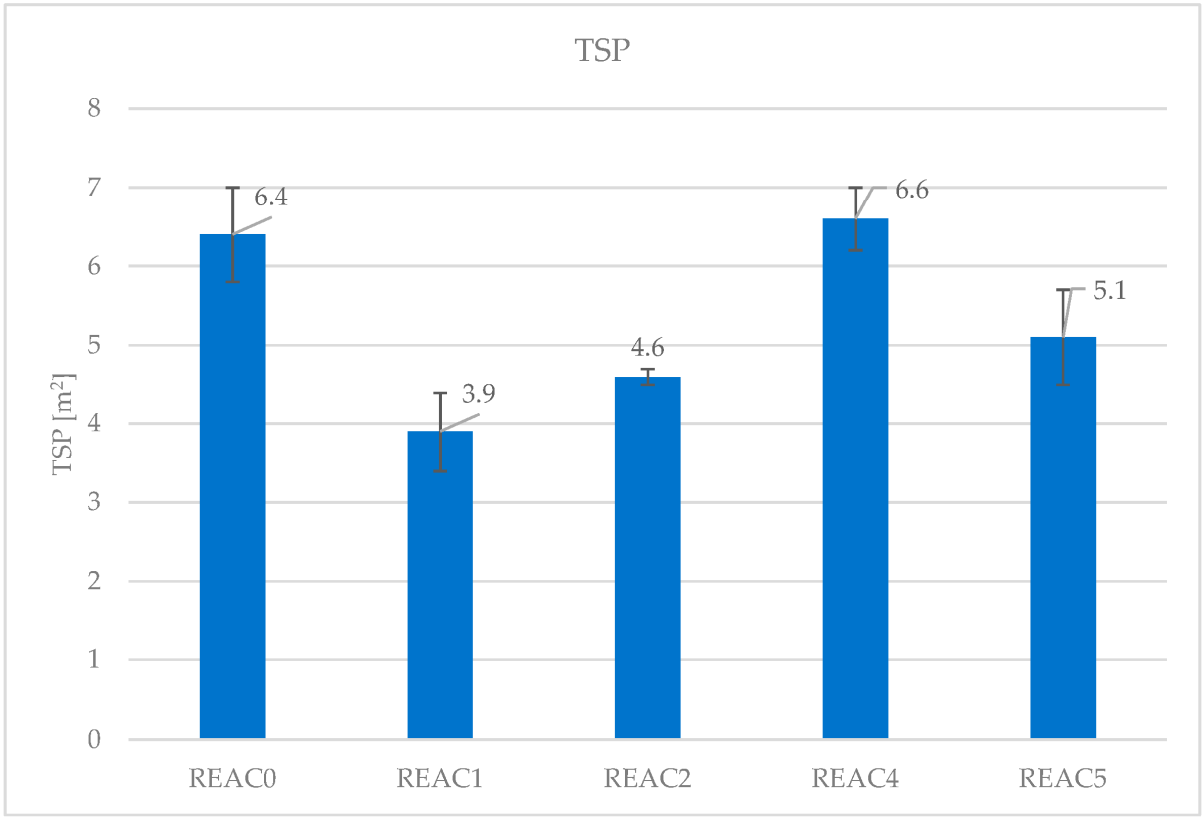

Figure 12. TSP of the formulations REAC0–5.

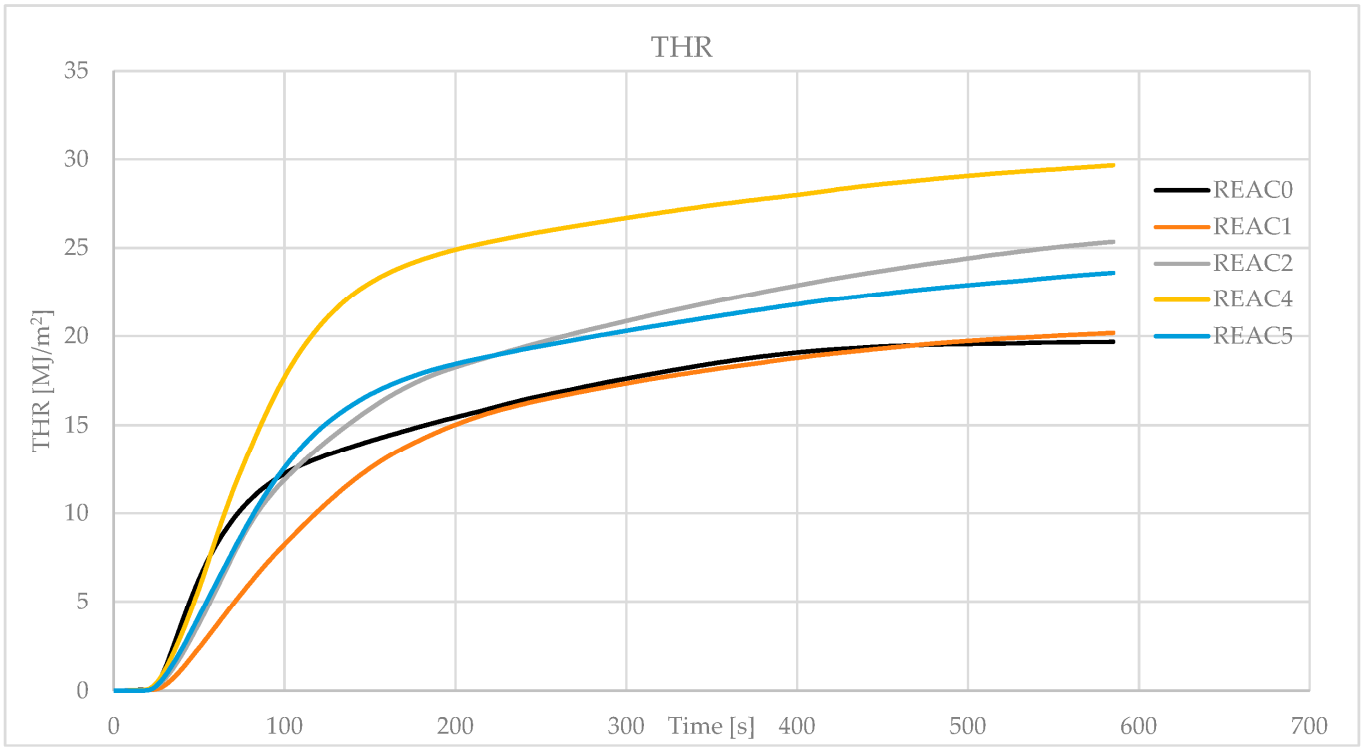

Figure 13. THR (t) of the formulations REAC0–5.

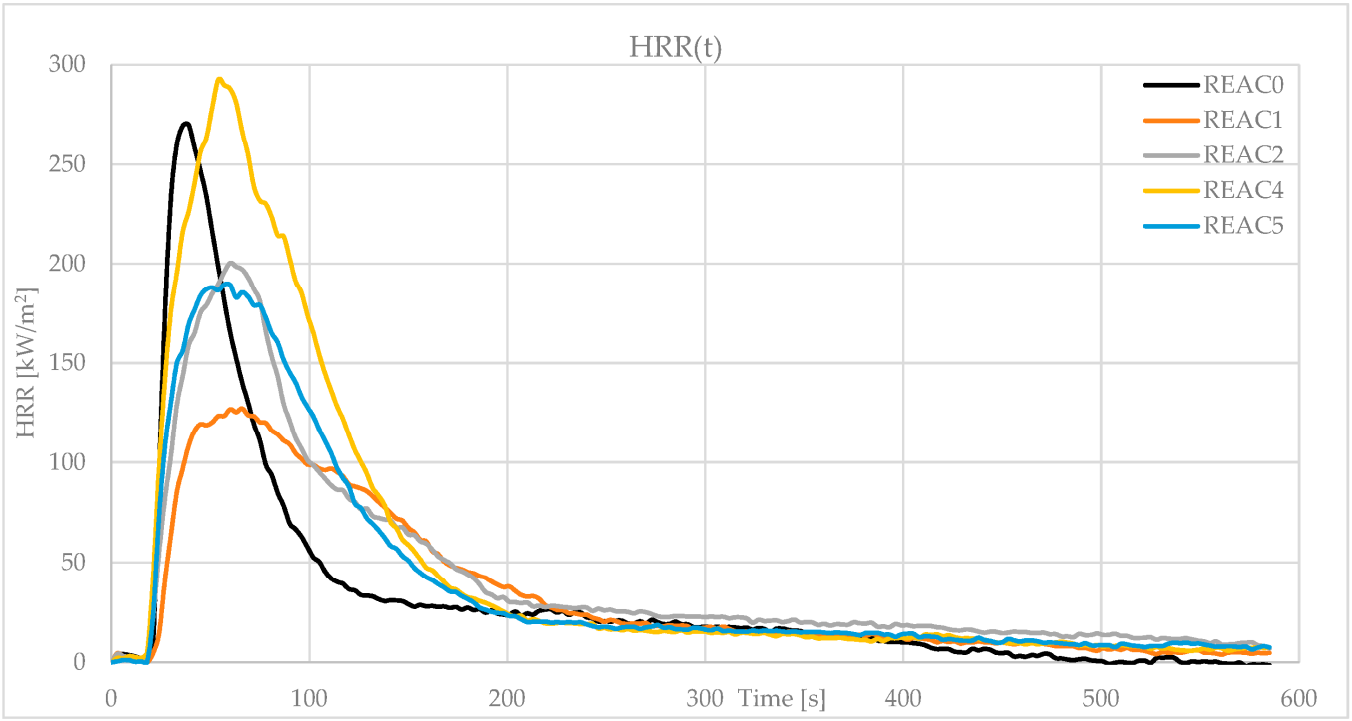

Figure 14. HRR (t) of the formulations REAC0–5.

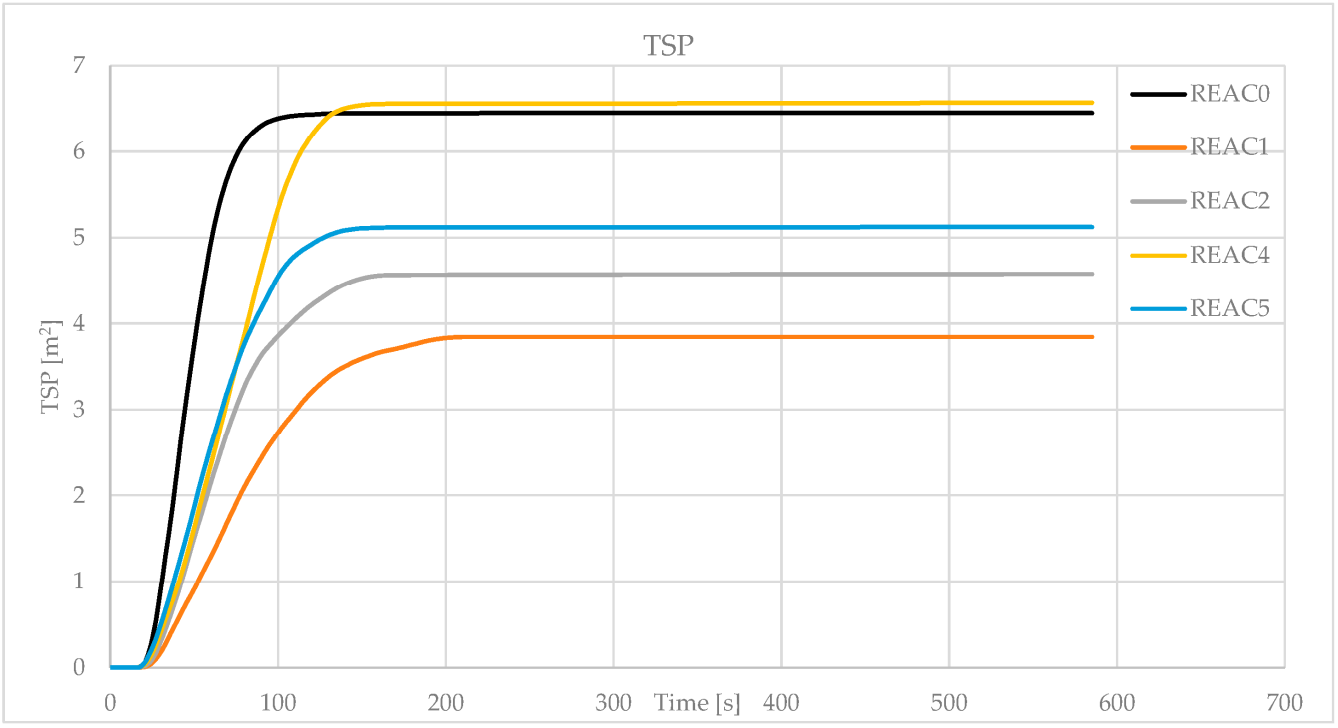

Figure 15. TSP(t) of the formulations REAC0–5.

REAC0 only has Reaguard B-FR/9211. pHRR is 270.4 kW/m^2 (Figure 9), and FIGRA is the highest in the series (Figure 10, 6239 W/s). THR is 18 MJ/m^2, releasing less heat than the others but at a higher speed (Figures 13 and 14). The smoke production evaluation shows that REAC0 has a 6.4 m^2 TSP (Figures 12 and 15). All cone calorimeter measurements indicate a performance improvement in the formulations with the addition of ATH and MDH—respectively, REAC1 and REAC2 (Figures 9–15). For example, FIGRA drops to

2616 W/s with ATH and 3986 W/s with MDH. Furthermore, TSP decreases respectively to 3.9 and 4.6 m^2. In particular, the formulations containing ATH and MDH show the best heat release and smoke production performance of the series. With potent acid scavengers at high temperatures in the condensed phase, such as Winnofil S, both the heat release and the smoke production parameters worsen compared to GCC (REAC5). For example, FIGRA for REAC4 in Figure 10 (6035 W/s) reaches almost the REAC0 rank (6239 W/s), while REAC5 FIGRA is much lower at 4316 W/s. That indicates how the HCl sequestration in REAC4 affects the fire performance of the compound. The same trends are highlighted regarding smoke measures, as indicated in Table 10, Figures 12 and 15. REAC4 has the highest TSP, 6.6 m^2, even more than REAC0. REAC5 containing GCC shows 5.1 m^2, being lower than REAC4 with UPCC. REAC1 and REAC2 give a more substantial smoke reduction, indicating that ATH and MDH work even in withstanding the smoke formation, probably releasing water and reducing the carbon particles, as described in Ref. [18].

The increase in smoke production due to HCl sequestration has also been evidenced by M. Piana in Refs. [37,38], where the smoke was measured as smoke density rating percentage (SDR%) according to ASTM D 2843.

Reaguard B-FR/9211 acts, in the condensed phase, as a flame retardant but also as a smoke suppressant.

The behavior of REAC4 clearly confirms that HCl scavenging also interferes with the action of the incipient Lewis acids in Reaguard B-FR/9211. Indeed, the sequestration of HCl prevents the formation of the potent Lewis acids (metal chlorides), and the pattern bringing to intramolecular rearrangement yielding benzene and soot becomes more probable than intermolecular reactions yielding matrix cross-linking.

4.4. Effect of Acid Scavenging on Measures from MCC

All specific HRR (T) curves show two stages. The first, centered around 260–360 °C, represents the energy released in the flame by the combustion of organic additives in the compound, particularly DINP, which evaporates in the gas phase, where it burns. Coming from intramolecular rearrangement of the polyene sequences, benzene is also combusted in the first stage. In the second stage, around 400–600 °C, the cross-linked polyene sequences release flammable moieties to the combustor, such as aliphatic and alkyl aromatic hydrocarbons, yielding a solid char in the pyrolizer [12]. The additives in the formulation decompose at different temperatures and with different energy, releasing gases such as CO_2 or water and impacting the shape of the specific HRR (T) curve.

The measures, usually taken into consideration in MCC shown in Table 10 and derived by the specific HRR (T), are the following:

- The maximum of the specific HRR (T) (Qmax). It is calculated for stages 1 and 2.
- The heat release temperature (Tmax) corresponds to the Qmax of stages 1 and 2.
- The heat release capacity (η_c) is the maximum rate of heat release divided by the heating rate.
- The specific (total) heat release (h_c). It is derived from the specific HRR (T) integral and represents the total heat released in the test. It calculates the contribution of h_c in stages 1 and 2.
- The specific heat of combustion of the fuel gases is the heat of combustion per gram of fuel burned in the combustor ($h_{c\ gas}$). It accounts for the energy released from the combustion of the fuels in the gas phase. It has also been split as the contribution from stages 1 and 2.
- The fire growth capacity (FGC) is defined in ASTM D7309-21 as a measure considering chemical processes responsible for igniting and burning combustible materials [26]. It is derived from other MCC measures such as η_c, ignition, and burning temperatures. FGC has been built considering the tendency of a material to ignite and spread the flame away from the fire source: ignitability and flame spread. FGC, a measure coming from a flammability micro-scale test, has been correlated to several other

measures from bench-scale tests used by Federal Aviation to discriminate levels of fire performances of the components in the cabin of an aircraft [26,39].
- Char yield. The initial and final weight ratios complete the measures in Table 10.

4.4.1. MCC of the Formulation of Table 1

REA1 is not flame-retarded, and it contains more combustible material than the others. It displays the highest Qmax, h_c, and FGC (Table 11). The addition of 3 phr of ATO in REA2 (LOI 29 $\%O_2$, Table 7) improves flame retardancy, and Qmax, h_c, and FGC decrease, while η_c is more or less comparable in all formulations. The effect of ATO seems more evident comparing LOI (Table 7, REA1 24 $\%O_2$ vs. REA2 29 $\%O_2$) and FIGRA values (Table 9, FIGRA, REA1 4187 W/s vs. REA2 3098 W/s) than in the MCC. That relies on the fact that ATO acts in the gas phase and does not contribute to the char formation in the pyrolysis process of MCC. ASTM D 7309 method A provides a temperature of 900 °C in the combustor. A temperature of 750 °C was chosen to make ATO's gas phase flame retardant action more evident.

REA7 with ATO and MDH (LOI 34.7 $\%O_2$, Table 7, FIGRA 1563 W/s, Table 9) shows how the synergistic action of two flame retardants can decrease the specific heat release in both stages (Table 11, Figure 16). Here, MDH dilutes the fuel in the flame and cools it down, decomposing endothermically between 300 °C and 330 °C. The decomposition of MDH perfectly tunes stage 1 of the decomposition/combustion of PVC compounds (Figure 16).

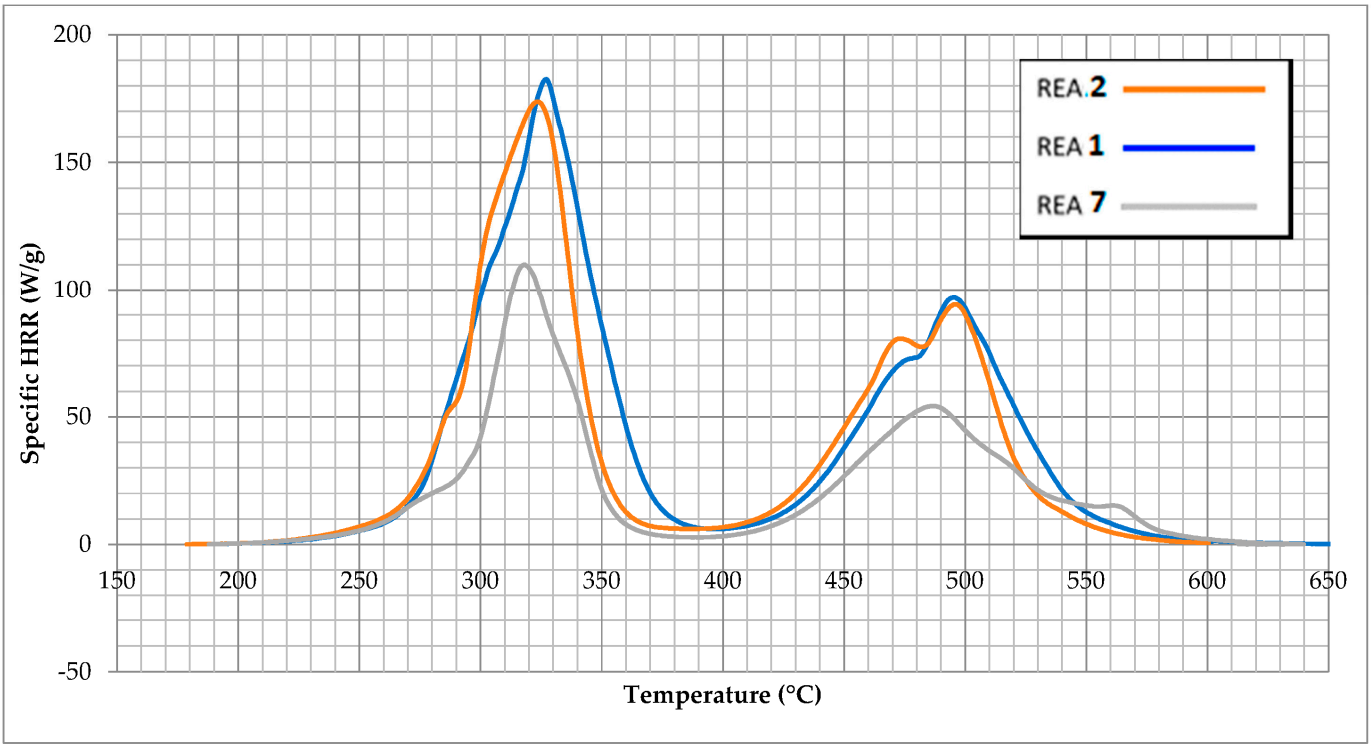

Figure 16. Comparison between REA1 (no flame retardants), REA2 (3 phr of ATO, 90 phr $CaCO_3$), and REA7 (3 phr of ATO and 90 phr of MDH).

Comparing the measures of REA3−5, it is clear how the HCl sequestration decreases the fire performance. REA5 with UPCC gives a higher FGC (104.72 J/g·K), Qmax (162.78 J/g), h_c (11.76 J/g), and $h_{c\ gas}$ (20.65 J/g) than REA3 and REA4. REA4, with a finer particle size $CaCO_3$, shows worst values than REA3, but the differences are near. REA6, containing a potent HCl scavenger, shows FGC 100.51 J/g·K, h_c (11.33 J/g), and $h_{c\ gas}$ (21.95 J/g) comparable with REA5. Qmax of REA6 is lower than REA5 due to a different impact that AS6-B has the shape of the specific HRR (T) curve. The action of the powerful

acid scavenger seems to delay the decomposition temperature and lower the peak of the specific HRR (T) of stage 1 (Table 9).

The $h_{c\ gas}$ shows strong reciprocity with HCl sequestration (Table 11, Figure 17).

The measure considers the energy released per gram of fuel gas combusted in the combustor. REA3 and REA4 containing GCC, which is less reactive with HCl, display overall lower values than REA5 formulated with UPCC. Therefore, REA5 releases more energy during the combustion, even though it releases more incombustible gases such as CO_2 in the first stage due to the fast reaction between HCl and UPCC. REA6 behaves similarly: a potent acid scavenger makes the gases more "flammable." In this case, 21.95 J/g is developed during the combustion of the gases, and the $h_{c\ gas}$ of REA5 and REA6 are even higher than the formulation without a flame retardant and with more plasticizer (REA1).

REA9 shows the synergistic combination of MDH and UPCC in scavenging HCl, lowering the smoke acidity (Table 5), but MDH also starts its function as a flame retardant through its endothermic decomposition releasing water at 300–330 °C. That explains the lower values of $h_{c\ gas}$ in the first stage in REA9 compared with REA5 (11.03 J/g vs. 12.86 J/g), showing that heat sink and fuel dilution are the main mechanisms reducing the $h_{c\ gas}$.

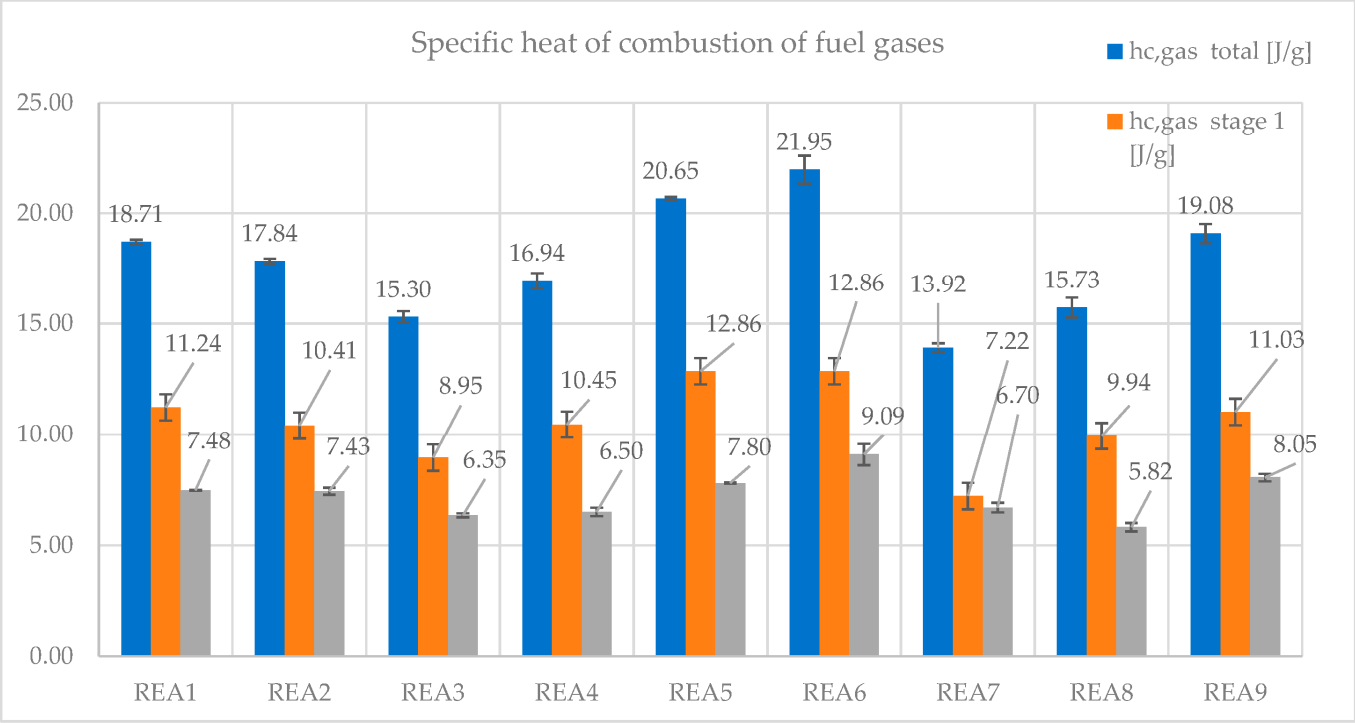

Figure 17. $h_{c\ gas}$ samples REA1–9. Blue column: total; orange: stage 1; grey: stage 2.

$h_{c\ gas}$ from stage 2 seems to worsen in the presence of acid scavengers (REA3, 6.35 J/g, REA4, 6.50 J/g, REA5, 7.80 J/g, REA6 9.09 J/g), and the comparison between REA7 and REA9 seems to confirm it (REA7, 6.70 J/g vs. REA9 8.05 J/g). The acid scavenger probably not only makes the fuel more flammable sequestrating HCl and worsening $h_{c\ gas}$ in the first stage (REA3, 8.93 J/g, REA4, 10.45 J/g, REA5, 12.86 J/g, REA6, 12.86 J/g), but somehow makes the condensation product from polyene sequences more prone to release flammable fuel (see Section 4.4 for entering more into detail of the topic).

4.4.2. MCC of the Formulation of Table 2

From the analysis of the MCC data of the formulations in Table 2 (Table 12), these comments follow. This set combines a powerful charring agent, Reaguard B-FR/9211, with flame retardant fillers such as ATH, MDH, GCC, and UPCC. Therefore, flame retardancy and smoke suppression act mainly in the condensed phase. REAC0 contains no filler

and 10 phr of Reaguard B-FR/9211. It shows the highest FGC, η_c, Q_{max} (102.68 J/g·K, 366.66J/g·K, 277.68 J/g), and the lower T_{max} (303.4 °C). It starts burning before the others and releases more heat. The addition of flame retardant fillers and acid scavengers to Reaguard B-FR/9211 in formulations REAC1, C2, C4, and C5 changes the shape of the specific HRR (T) curve. However, no solid correlation can be established by analyzing FGC, ηc, Q_{max}, T_{max}, and smoke acidity, possibly due to many interplaying factors that are not easily separated as linear functions of single measurable parameters. The only measures of extreme interest that bring correlation are h_c (Figure 18, Table 12) and $h_{c\ gas}$ (Figure 19, Table 12).

In the formulation REAC4 with UPCC, the heat released in the first stage is higher than in REAC5, containing trivial GCC (Figure 18, Table 12). REAC4 shows an h_c of 11.32 J/g, which is much more than REAC5, 9.41 J/g. In the second stage, REAC4 reaches h_c values close to REAC0 (3.98 J/g vs. 4.19 J/g).

REAC4 contributes more to heat in the first stage than in the second (Figure 18). The UPCC in REAC4 scavenges HCl, worsening the item's fire behavior.

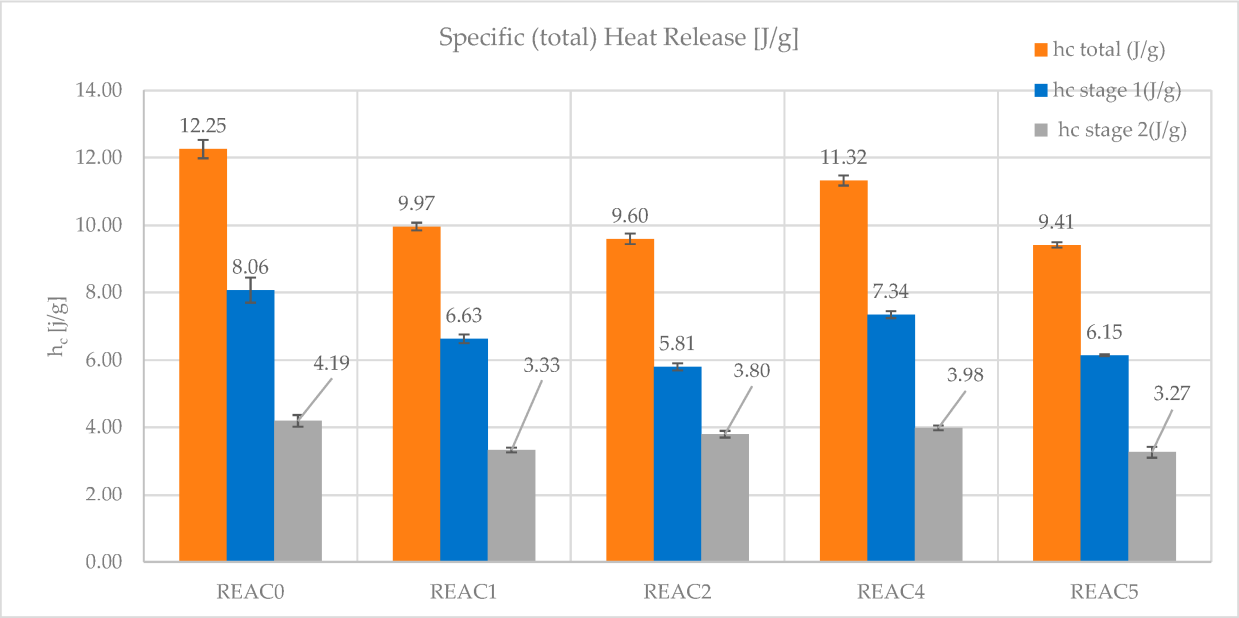

Figure 18. Comparison of h_c in REAC0–REAC5. Specifically, REAC4 contains an HCl scavenger, while REAC5 a trivial GCC.

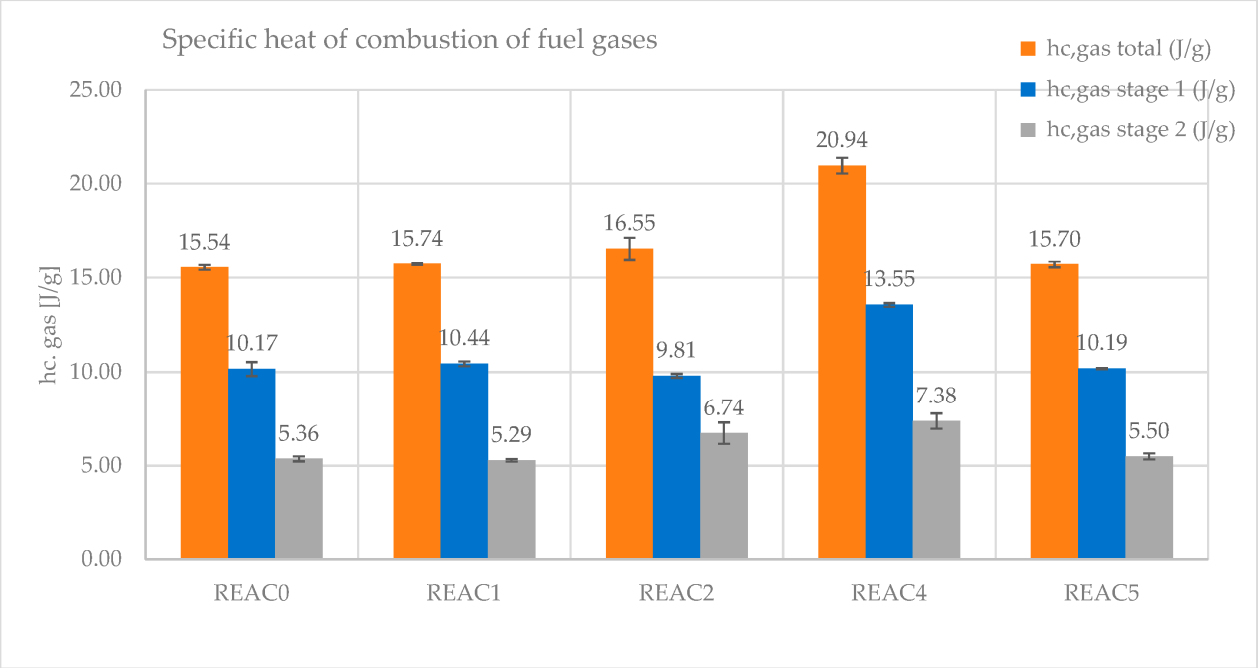

Figure 19. Comparison of $h_{c\ gas}$ in REAC0–REAC5. Specifically, REAC4 contains an HCl scavenger, while REAC5 a trivial GCC.

$h_{c\ gas}$ again gives much information on HCl scavenging. REAC4 with UPCC brings a $h_{c\ gas}$ total of 20.94 J/g against 15.70 J/g of the formulation containing GCC, REAC5 (Figure 19). The contribution is high in the first stage (REAC4, 13.55 J/g vs., REAC5, 10.19 J/g) but also in the second (REAC4, 7.38 J/g vs., REAC5, 5.50 J/g).

h_c and $h_{c\ gas}$ clearly indicate that in REAC4, the sequestration of HCl enhances the flame's energy. Additionally, in stage 2, REAC4 releases more energy than REAC5. Here, the heat comes from fuel combustion from the char in stage 2. It can be viewed as an indirect measure of the consistency of the char. If a powerful acid scavenger captures most of the HCl, it prevents the formation of potent Lewis acids through the reaction between HCl and incipient Lewis acids used in flame retardants and smoke suppressants such as Reaguard B-FR/9211. Therefore, there will be less cross-linking of the polyene sequences and fewer condensation products. What is left will be more prone to lose moieties to the gas phase, which justifies the higher $h_{c\ gas}$ in stage 2 of REAC4 than REAC5 (Figure 19). Furthermore, 9 explains that without potent Lewis acids, the intramolecular reactions of cis–trans polyene sequences yielding benzene will be more probable. As a result, that will bring more soot and smoke, as cone calorimetry actually confirmed.

The analysis of the specific HRR (T) curves in Figure 20 shows how, when CGG is present in the first stage, the combustion starts earlier (REAC5 325 °C vs. REAC4 334.1 °C), with a quicker speed (η_c REAC5 287.92 J/g·K, vs. REAC4 229.07 J/g·K), but the curve is sharper, declining fast to lower specific HRR (T) values.

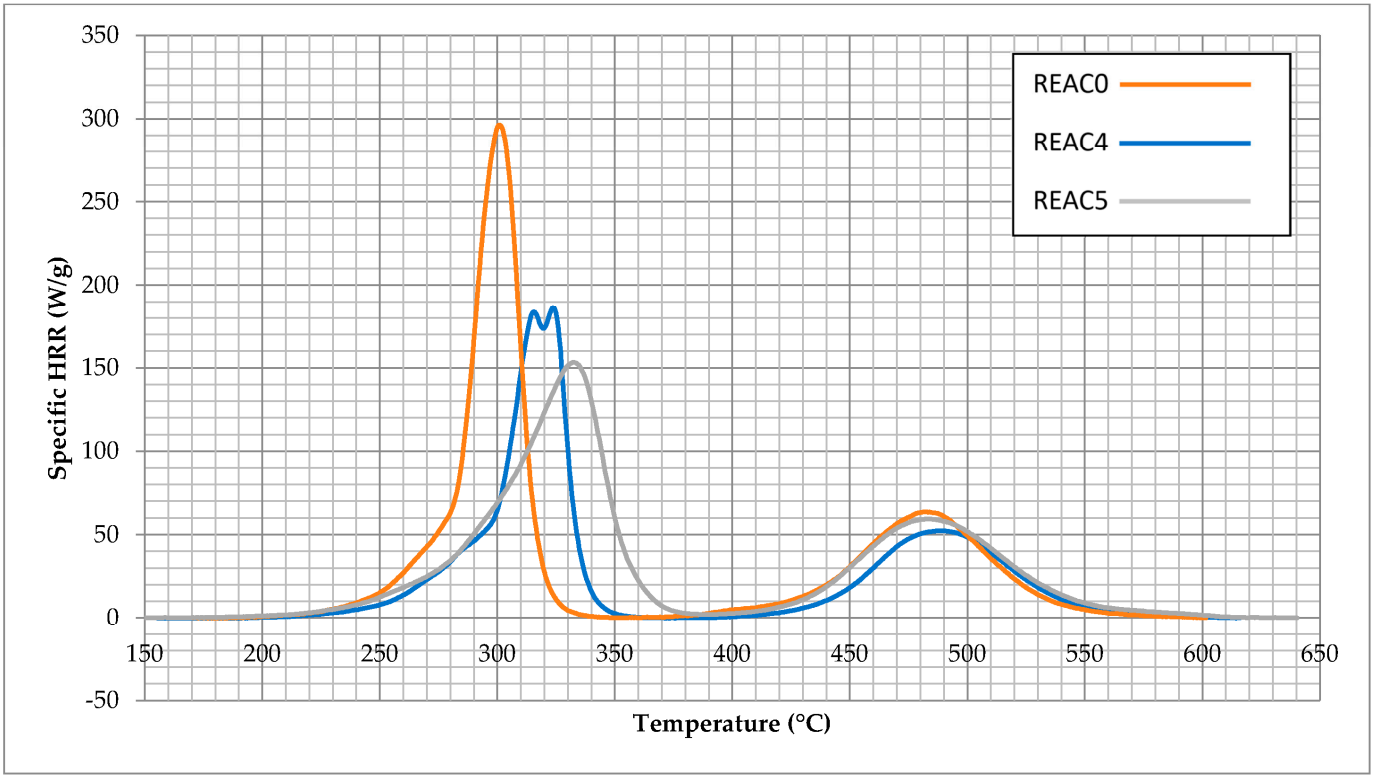

Figure 20. Specific HRR of REAC0 (containing only Reaguard B−FR/9211), REAC4 (containing Reaguard B−FR/9211 and Winnofil S), and REAC5 (containing Reaguard B−FR/9211 and Atomfor S).

The analysis of the data related to REAC2 and REAC3 is also interesting. REAC0 shows the highest value of h_c (12.25 J/g, Figure 12). The addition of flame retardant fillers shows a strong reduction of h_c (REAC1, 9.97 J/g, and REAC2, 9.60 J/g). ATH works better in the second stage, while MDH is in the first. The shapes of the HRR (T) curve of REAC1 and REAC2 are completely different (Figure 21). They differ from REAC0 mainly in η_c (REAC0 366.66 J/g·K, REAC1 212.13, REAC2 259.66 J/g·K, Table 12), in first stage Q_{max} (REAC0, 277.68 J/g, REAC1 123.38 J/g, REAC2 196.29 J/g, Table 12), and T_{max} (REAC0, 303.4 °C, REAC1 326.5 °C, REAC2 314.8 °C, Table 12). Both show a marked flame retardance but with different behavior. While in the second stage Q_{max} and the h_c are lower in REAC1 than REAC2, in stage 1, REAC1 starts the combustion at lower temperatures but with a milder slope than REAC2. In the end, the area of the HRR (T) curve in stage 1 is higher in REAC1, but the speed to the peak, η_c, is higher in REAC2 than REAC1 (Figure 21, Table 12). The reasons are probably in the different temperatures at which ATH and MDH work. ATH decomposes at 190–210 °C, making free water. Probably, water helps the expulsion of plasticizer in the gas phase (probably promoting hydrolysis), but this should be clarified with other instrumentation such as TGA-FTIR.

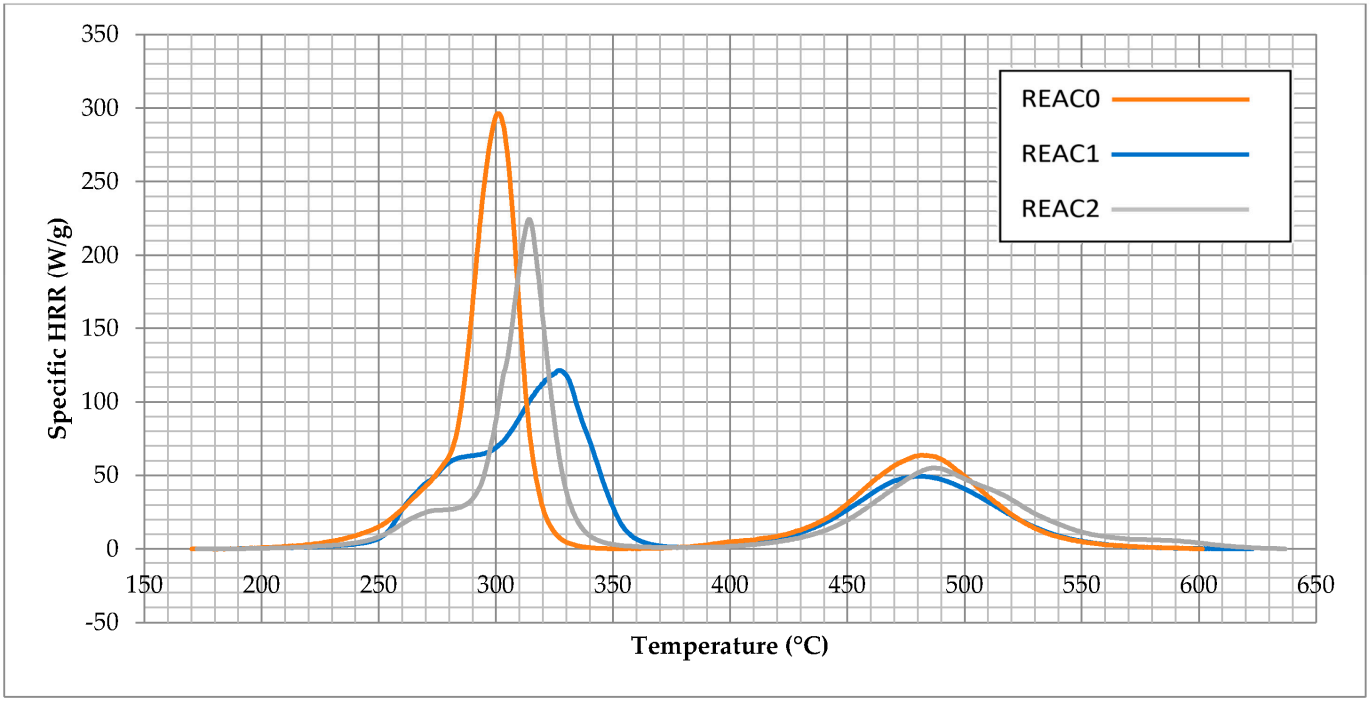

Figure 21. Specific HRR of REAC0 (containing only Reaguard B−FR/9211), REAC1 (containing Reaguard B−FR/9211 and ATH), and REAC2 (containing Reaguard B−FR/9211 and MDH).

If the hypothesis is correct, most combustible fuel from plasticizer moieties will burn at a lower temperature. Water vapor impedes a quick heat release, and the curve flattens and enlarges when the primary flame retardant in the gas phase is wholly consumed.

The data in the second stage show how h_c and $h_{c\ gas}$ decrease more in REAC1 than in REAC2 (Table 12). That is reflected in a more consistent char residue of REAC1, as shown in Scheme 1.

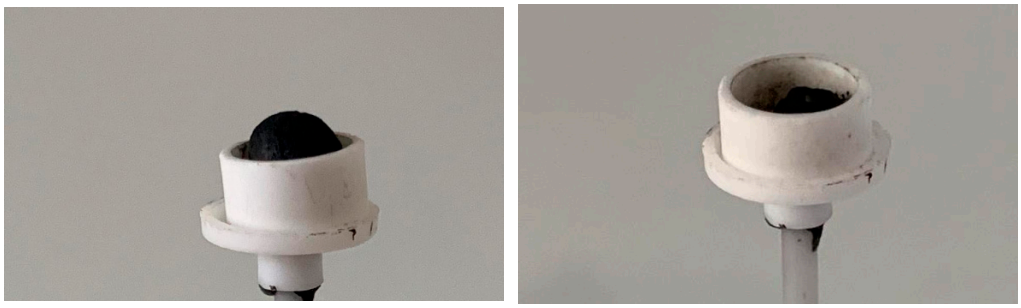

Scheme 1. Left: REAC1 char residue; right: REAC2 char residue.

5. Conclusions

Thermal stability is a measure that must be evaluated in the process stage of PVC items and their useful life. Thermal decomposition of the item must be considered in case of fire when specific additives in the item can affect the chemistry of the flame retardancy and smoke suppression in the condensed and gas phases, contributing negatively or positively to heat release and smoke production. The decomposition/combustion stage can be followed through MCC, plotting the specific HRR versus T, and the shape of HRR (T) is affected by the additives used in the PVC compound. In the decomposition/combustion stage, HCl reaches the gas phase inhibiting the reactions sustaining the flame's energy. However, HCl also creates potent Lewis acids in the condensed phase with the right additives, promoting char formation and decreasing the heat release rate and smoke production.

Acid scavengers at high temperatures trap most of the released HCl, affecting the fire performances of the items; since acid scavengers trap a significant amount of HCl in the condensed phase, HCl cannot reach the gas phase, and therefore its scavenging of the radicals ·OH and ·H in the flame is hindered. Furthermore, the lack of HCl impedes the formation of actual Lewis acid that is responsible for the charring mechanism, passing through the cross-linking of the polyene sequences. Without potent Lewis acids, the more favorable pathway during decomposition is the intramolecular rearrangement of polyene sequences yielding to the benzene formation and, therefore, a substantial increase in smoke production and reduction of flame retardancy. Indeed, without potent Lewis acids, the char is more fragile and prone to release fuels sustaining the flame's energy.

The data also confirm that the actual char promoters are the metal chlorides from the incipient Lewis acids in Reaguard B-FR/9211, as Montaudo showed in Ref. [10], where the polyacetylene thermal decomposition in the presence of metal oxides was explored.

Low-smoke acidity compounds can be essential to introduce PVC cables in classes a_2 or a_1 in high- and medium-risk locations [40]. Such compounds will lose flame retardancy and increase smoke production as much as HCl scavenging is efficient. That issue paves the way for developing a new generation of flame retardants and smoke suppressants working efficiently in low-smoke acidity conditions.

Supplementary Materials: The following are available online at https://www.mdpi.com/article/10.3390/fire6070259/s1, Table S1: commercial additives.

Author Contributions: Conceptualization, G.S.; methodology, G.S., F.D., I.B., C.B., L.M., and E.S.; writing—original draft preparation, G.S.; writing—review and editing, G.S., F.D., I.B., C.B., L.M., and E.S. All authors have read and agreed to the published version of the manuscript.

Funding: This research received no external funding.

Institutional Review Board Statement: Not applicable.

Acknowledgments: The authors would like to acknowledge Ing. Carlo Ciotti, Ing. Marco Piana, all PVC Forum Italia, and the PVC4cables staff.

Conflicts of Interest: The authors declare that there is no conflict of interest regarding the publication of this paper.

Abbreviations

PVC	Poly(vinyl chloride);
HCl	Hydrogen chloride;
EU	European Union;
CPD	Construction Product Directive;
CPR	Construction Product Regulation;
UPCC	Precipitated Calcium Carbonate;
GCC	Ground Calcium Carbonate;
Phr	Part per Hundred Resin;
DINP	Di Iso Nonyl Phthalate;
ESBO	Epoxidized Soy Bean Oil;
COS	Calcium Organic Stabilizer;
DDW	Double Deionized Water;
M	Mean;
SD	Standard Deviation;
CV	Coefficient of variation;
MCC	Micro Combustion Calorimetry

Appendix A. A Schematic Diagram of the Sample Preparation and Testing Process

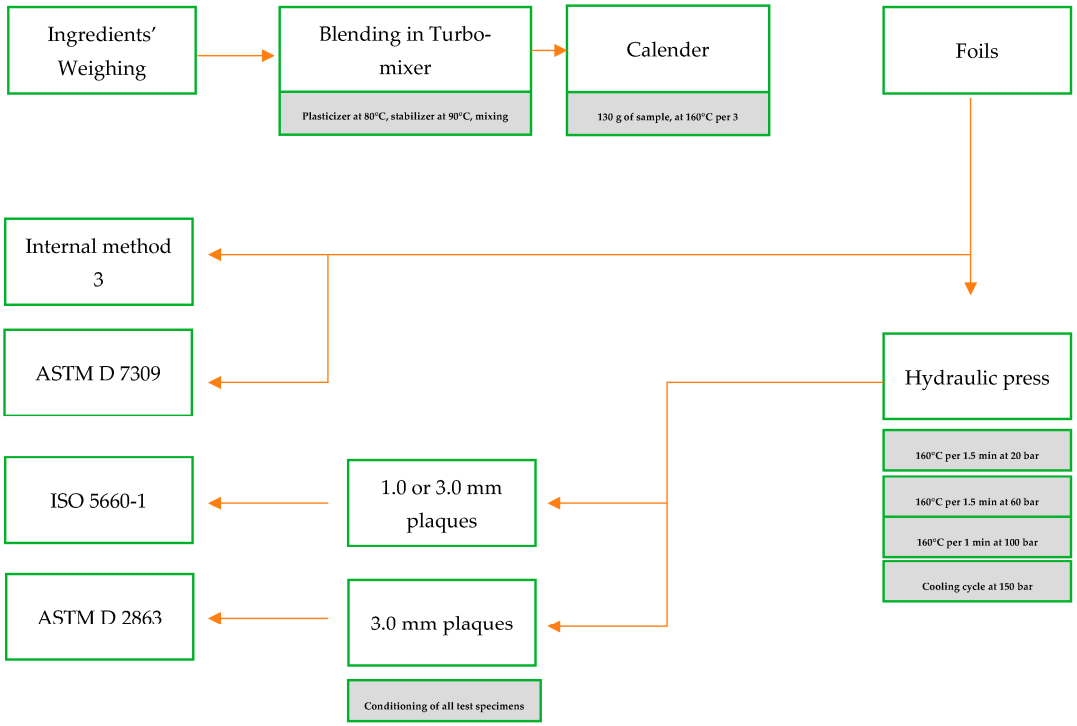

Figure A1. A schematic diagram of the sample preparation.

Figure A2. A schematic diagram of the testing process and main conditions.

References

1. Hjertberg, T.; Sörvik, E.M. Thermal Degradation of PVC. In *Degradation and Stabilisation of PVC*; Owen, E.D., Ed.; Springer: Dordrecht, The Netherlands, 1984. [CrossRef]
2. Starnes, W.H. How and to What Extent Are Free Radicals Involved in the Nonoxidative Thermal Dehydrochlorination of Poly(vinyl chloride). *J. Vinyl Addit. Technol.* **2012**, *18*, 71–75. [CrossRef]
3. Starnes, W.H.; Ge, X. Mechanism of Autocatalysis in the Thermal Dehydrochlorination of Poly(vinyl chloride). *Macromolecules* **2004**, *37*, 352–359. [CrossRef]
4. Starnes, W.H.; Wallach, J.A.; Yao, H. Six-Center Concerted Mechanism for Poly(vinyl chloride) Dehydrochlorination. Requiescat in Pace? *Macromolecules* **1996**, *29*, 7631–7633. [CrossRef]
5. Starnes, W.H. Structural and mechanistic aspects of the thermal degradation of poly(vinyl chloride). *Prog. Polym. Sci.* **2002**, *27*, 2133–2170. [CrossRef]
6. Lynda, P.B. The Dehydrochlorination Mechanism of the Internal Allylic Chloride Structure in Poly(Vinyl Chloride). Dissertations, Theses, and Masters Projects. Master's Thesis, William & Mary, Williamsburg, VA, USA, 2000. [CrossRef]
7. Schartel, B.; Hull, T.R. Development of fire-retarded materials—Interpretation of cone calorimeter data. *FAM* **2007**, *31*, 327–354. [CrossRef]
8. Starnes, W.H.; Edelson, D. Mechanistic Aspects of the Behavior of Molybdenum(VI) Oxide as a Fire-Retardant Additive for Poly(vinylvinyl chloride). *Macromolecules* **1979**, *12*, 797–802. [CrossRef]
9. Starnes, W.H.; Wescott, L.D.; Reents, W.D.; Cais, R.E.; Villacorta, G.M.; Plitz, I.M.; Anthony, L.J. Mechanism of poly(vinyl chloride) fire retardance by molybdenum(vi) oxide. Further evidence in favor of the Lewis acid theory. In *Polymer Additives. Polymer Science and Technology*; Kresta, J.E., Ed.; Springer: Boston, MA, USA, 2007; Volume 26, pp. 237–248. [CrossRef]
10. Montaudo, G.; Puglisi, C. Evolution of aromatics in the thermal degradation of poly(vinyl chloride): A mechanistic study. *Polym. Degrad. Stab.* **1991**, *33*, 229–262. [CrossRef]
11. Wu, C.H.; Wu, C.H.; Chang, C.Y.; Hor, J.L.; Shih, S.M.; Chen, L.W.; Chang, F.W. Two-stage pyrolysis model of PVC. *Can. J. Chem. Eng.* **1994**, *72*, 644–650. [CrossRef]
12. Anthony, G.M. Kinetic and Chemical Studies of Polymer Cross-Linking Using Thermal Gravimetry and Hyphenated Methods. Degradation of Polyvinylchloride. *Polym. Degrad. Stab.* **1999**, *64*, 353–357. [CrossRef]
13. O'Mara, M.M. Combustion of PVC. *Pure Appl. Chem.* **1977**, *49*, 649–660. [CrossRef]
14. Ballistreri, A.; Foti, S.; Maravigna, P.; Montaudo, G.; Scamporrino, E. Effect of metal oxides on the evolution of aromatic hydrocarbons in the thermal decomposition of PVC. *J. Polym. Sci. Polym. Chem. Ed.* **1980**, *18*, 3101–3110. [CrossRef]
15. Fenimore, C.P.; Martin, F.J. The Mechanisms of Pyrolysis, Oxidation, and Burning of Polymers. In *NBS Special Publication 357*; Wall, L.A., Ed.; Executive Agency: Brussels, Belgium, 1972; pp. 159–170. Available online: https://nvlpubs.nist.gov/nistpubs/Legacy/SP/nbsspecialpublication357.pdf (accessed on 1 June 2023).
16. Marcilla, A.; Beltrán, M. Kinetic models for the thermal decomposition of commercial PVC resins and plasticizers studied by thermogravimetric analysis. *Polym. Degrad. Stab.* **1996**, *53*, 251–260. [CrossRef]
17. Laoutid, F.; Bonnaud, L.; Alexandre, M.; Lopez-Cuesta, J.-M.; Dubois, P. New prospects in flame retardant polymer materials: From fundamentals to nanocomposites. *Mater. Sci. Eng. Rep.* **2009**, *63*, 100–125. [CrossRef]
18. Edelson, D.; Kuck, V.J.; Lum, R.M.; Scalco, E.; Starnes, W.H.; Kaufman, S. Anomalous behavior of molybdenum oxide as a fire retardant for polyvinyl chloride. *Combust. Flame* **1980**, *38*, 271–283. [CrossRef]
19. Pike, R.; Starnes, W.H.; Jeng, J.P.; Bryant, W.S.; Kourtesis, P.; Adams, C.W.; Bunge, S.D.; Kang, Y.M.; Kim, A.S.; Kim, J.H.; et al. Low-Valent Metals as Reductive Cross-Linking Agents: A New Strategy for Smoke Suppression of Poly(vinyl chloride). *Macromolecules* **1997**, *30*, 6957–6965. [CrossRef]
20. Li, B.; Wang, J. A Cone Calorimetric Study of Flame Retardance and Smoke Emission of PVC. I. The Effect of Cuprous and Molybdic Oxides. *J. Fire Sci.* **1997**, *15*, 341–357. [CrossRef]
21. Li, B. A study of the thermal decomposition and smoke suppression of poly(vinyl chloride) treated with metal oxides using a cone calorimeter at a high incident heat flux. *Polym. Degrad. Stab.* **2002**, *78*, 349–356. [CrossRef]
22. Morley, J.C.; Grossman, R.F. Flame Retardants and Smoke Suppressants. In *Handbook of Vinyl Formulating*, 2nd ed.; Grossman, R.F., Ed.; John Wiley & Sons Inc.: Hoboken, NJ, USA, 2007; pp. 403–414. [CrossRef]
23. Sarti, G. A New Perspective on Hydrogen Chloride Scavenging at High Temperatures for Reducing the Smoke Acidity of PVC Cables in Fires. I: An Overview of the Theory, Test Methods, and the European Union Regulatory Status. *Fire* **2022**, *5*, 127. [CrossRef]
24. Sarti, G. A New Perspective on Hydrogen Chloride Scavenging at High Temperatures for Reducing the Smoke Acidity of PVC Cables in Fires. II: Some Examples of Acid Scavengers at High Temperatures in the Condensed Phase. *Fire* **2022**, *5*, 142. [CrossRef]
25. *ASTM D 2863:2019*; Standard Test Method for Measuring the Minimum Oxygen Concentration to Support Candle-Like Combustion of Plastics (Oxygen Index). ASTM International: West Conshohocken, PA, USA, 2019. Available online: www.astm.org (accessed on 1 June 2023).
26. *ISO 5660-1:2015*; Reaction-to-Fire Tests—Heat Release, Smoke Production and Mass Loss Rate—Part 1: Heat Release Rate (Cone Calorimeter Method) and Smoke Production Rate (Dynamic Measurement). ISO: Geneva, Switzerland, 2015. Available online: https://www.iso.org/standard/57957.html (accessed on 1 June 2023).

27. *ASTM D 7309:2019*; Standard Test Method for Determining Flammability Characteristics of Plastics and Other Solid Materials Using Microscale Combustion Calorimetry. ASTM International: West Conshohocken, PA, USA, 2019. Available online: www.astm.org (accessed on 1 June 2023).
28. Kipouros, G.J.; Sadoway, D.R. A thermochemical analysis of the production of anhydrous $MgCl_2$. *J. Light Met.* **2001**, *1*, 111–117. [CrossRef]
29. Galwey, A.K.; Laverty, G.M. The thermal decomposition of magnesium chloride dihydrate. *Thermochim. Acta* **1989**, *138*, 115–127. [CrossRef]
30. Commercial PCC Purchased by Imerys. Available online: https://www.imerys-performance-minerals.com/system/files/2021-02/DATPCC_Winnofil_S_LSK_EN_2019-07.pdf (accessed on 1 June 2023).
31. *EN 60754-2:2014/A1:2020*; Test on Gases Evolved during Combustion of Materials from Cables—Part 2: Determination of Acidity (by pH Measurement) and Conductivity. CENELEC: Brussels, Belgium, 2020.
32. *EN 60754-1:2014/A1:2020*; Test on Gases Evolved during Combustion of Materials from Cables—Part 1: Determination of the Halogen Acid Gas Content. CENELEC: Brussels, Belgium, 2020.
33. *EN 138523:2022;* Reaction to Fire Tests for Building Products—Building Products Excluding Floorings Exposed to the Thermal Attack by a Single Burning Item. CEN: Brussels, Belgium, 2022. Available online: https://store.uni.com/en-13823-2020-a1-2022 (accessed on 1 June 2023).
34. Bassi, I. Characterization of PVC Compounds and Evaluation of Their Fire Performance, Focusing on the Comparison between EN 60754-1 and EN 60754-2 in the Assessment of the Smoke Acidity. Master's Thesis, University of Bologna, Bologna, Italy, 2021. Available online: https://www.pvc4cables.org/images/assessment_of_the_smoke_acidity.pdf (accessed on 1 June 2023).
35. Hirschler, M. Poly(vinyl chloride) and its fire properties. *FAM* **2017**, *41*, 993–1006. [CrossRef]
36. Babrauskas, V.; Richard, D. Peacock, Heat release rate: The single most important variable in fire hazard. *Fire Saf. J.* **1992**, *18*, 255–272. [CrossRef]
37. Sarti, G.; Piana, M. New formulations and test comparison for the classification of PVC cables under EU regulation n 305/2011 for construction products. In Proceedings of the AMI Cables 2019, Duesseldorf, Germany, 5–7 March 2019.
38. Sarti, G.; Piana, M. PVC cables and smoke acidity: A review comparing performances of old and new compounds. In Proceedings of the AMI Cables 2020, Duesseldorf, Germany, 3–5 March 2020.
39. DOT/FAA/TC-22/22 Federal Aviation Administration William, J. Hughes Technical Center Aviation Research Division Atlantic City International Airport New Jersey 08405. Final Report Microscale Flammability Criterion for Constituents of Aircraft Cabin Materials. 2022. Available online: https://www.fire.tc.faa.gov/pdf/TC22-22.pdf (accessed on 1 June 2023).
40. Sarti, G.; Piana, M. PVC in cables for building and construction. Can the "European approach" be considered a good example for other countries? *Acad. Lett.* **2022**, 5453. [CrossRef]